Anomalous scaling and Lee-Yang zeros in self-organized criticality

B. Cessac and J. L. Meunier
Institut Non Linéaire de Nice, 1361 Route des Lucioles, 06500 Valbonne, France
(Received 25 July 2001; revised manuscript received 12 November 2001; published 28 February 2002)

We show that the generating functions of probability distributions in self-organized criticality (SOC) models exhibit a Lee-Yang phenomenon [Phys. Rev. **87**, 404 (1952)]. Namely, their zeros pinch the real axis at $z=1$, as the system size goes to infinity. This establishes a new link between the classical theory of critical phenomena and SOC. A scaling theory of the Lee-Yang zeros is proposed in this setting.

DOI: 10.1103/PhysRevE.65.036131 PACS number(s): 05.65.+b, 02.10.De, 02.90.+p, 05.45.−a

INTRODUCTION

In 1988, Bak, Tang, and Wiesenfeld (BTW) [1] proposed a mechanism in which a dynamical system reaches ''spontaneously'' a stationary state with some features reminiscent of a critical state. More precisely, by its only internal reorganization in reaction to (stationary) external perturbations, a system organizes into a state with scale invariance and power law statistics. This effect, called self-organized criticality (SOC), was quite unexpected, since usually the critical state of a thermodynamic system needs a fine tuning of some control parameter (temperature, magnetic field, etc. . . .) which is at first sight absent from the model introduced by BTW and from the many variants proposed later [2,3]. Furthermore, the stationary regime corresponds to a nonequilibrium situation where the (stationary) flux of external perturbation is dissipated in the bulk or at the boundaries, generating a constant flux through the system. As a consequence, one generally believes that the usual equilibrium statistical mechanics treatments using the concepts of Gibbs measure, free energy, etc. . . . cannot be applied for the analysis of SOC systems.

On the other hand, it is also believed that concepts like universality classes, critical exponents, order parameter, etc. . . . , borrowed from the equilibrium statistical mechanics of phase transitions, are still relevant in SOC. Actually, the identification of universality classes is one of the main goals in the SOC literature. However, since these concepts are not defined via a thermodynamic analysis, alternative definitions are used. The dynamics of SOC systems occurring in chain reactions or ''avalanchelike'' events, a set of observables characterizing the avalanches, size (s), duration (t), area (a), etc. . . . , are defined. Fix such an observable, say N, and compute the related probability $P_L(n) \stackrel{\text{def}}{=} \text{Prob}(N=n)$ at stationarity for a system of characteristic size L. The numerical simulations show that the graph of $P_L(n)$ exhibits a power law behavior over a finite range, with a cutoff corresponding to finite size effects. As L increases the power law range increases. This leads to the conjecture that as $L \to \infty$, $P_L(n)$ converges to a probability distribution $P^*(n)$, with a power law tail having an exponent τ_n called the *critical exponent* of the observable n. It seems commonly admitted in the SOC community that a classification of the models can be made by the knowledge of their critical exponents (''universality classes''). Consequently, a large effort has been devoted to the computation of these quantities.

Considerably less efforts have been made to establish a clear foundation of the basic SOC concepts and to clarify their connection to their classical statistical mechanics counterpart [4,5]. Clearly, this is a hard task since even preliminary notions like ''state'' or ''thermodynamic limit,'' though intuitively clear, suffer from a lack of precise mathematical definition in this setting. In discrete automata like the BTW model [6] the state is the unique ergodic probability measure, μ_L, of a discrete Markov chain, finite when L is finite. In continuous dynamical systems like the Zhang model [7] there exists typically infinitely many ergodic measures and therefore one has to add additional constraints to define the state μ_L in a nonambiguous way [8–10]. The probability distributions P_L, for the observables $a,s,t,\ldots$ are directly obtained from μ_L [8,10] but they contain less information. The observable a,s,t are simply indicators of the dynamics. There is no *a priori* reason to believe that the knowledge of $P_L(s),P_L(a),P_L(t)$ or even of the joint probability $P_L(a,s,t)$ gives all the relevant (that is, allowing us to classify the models into universality classes) information about the state μ_L.

The thermodynamic limit $L \to \infty$ and the supposed ''convergence'' of μ_L to a ''critical state'' poses deeper problems since even the proof that there exists *indeed* a limiting state and that the probability distribution of avalanche observables are still defined in this limit remains to be done, for most models. The usual classical statistical mechanics constructions of the thermodynamic limit like the Dobrushin-Landford-Ruelle's (DLR) [11] cannot be directly applied because of the *a priori* absence of a Gibbs formalism. On the other hand, the methods used in interacting particle systems, allowing us to define the dynamics in the thermodynamic limit, on the basis of the Hille-Yoshida theorem and the properties of Feller processes, requires locality conditions which are broken in the SOC model. One has then to develop new ideas for non-Fellerian Markov processes and this has only been done in a few examples [12].

But one of the main problem is *the treatment of the data obtained from finite size systems simulations itself* and the extrapolation to the $L \to \infty$ limit. Indeed, though it was believed in the earlier SOC papers that this extrapolation can be handled by classical finite-size scaling [13], further investigations proposed alternative scaling [14–16] and, at the

moment, there is no agreement on which scaling form applies. Consequently, a lot of efforts have yet to be devoted to the understanding and analysis of SOC models.

Though the analogy between self-organized criticality and usual critical phenomena is the core of the SOC paradigm, it is remarkable that, up to now, some well developed techniques of analysis of critical phenomena have not been adapted to the study of SOC models. A phase transition has different manifestation. It is in particular characterized by a singularity of the thermodynamic potential (free energy, pressure). At a phase transition point, and for suitable interactions, the free energy, which is the generating function of the cumulants, exists in the thermodynamic limit but it is not analytic (in a kth order phase transition it is $\mathcal{C}^{k-1}$ but not $\mathcal{C}^k$). In many examples, the failure of analyticity is manifested by the Lee-Yang phenomenon [17]. For finite size systems the partition function is a polynomial in a variable z which typically depends on control parameters like the temperature or the external field. Since all coefficients are positive there is no zero on the positive real axis. However, in the thermodynamic limit, at the critical point, some zeros pinch the real axis at $z=1$, leading to a singularity in the free energy. The finite-size scaling properties of the leading zeros and of the density of zeros near to $z=1$ determine the order of the transition [18] and also the critical exponents in the case of a second order phase transition [19].

A natural question is whether there exists a similar property in SOC, namely can we exhibit a ''free-energy-like'' function, developing singularities in a similar way in the infinite lattice size limit. Though there exists a huge literature about the Lee-Yang zeros, there is, to the best of our knowledge, no attempt to study self-organized criticality from this point of view. In this paper, we show that the cumulants generating function of the probability distribution of the observables $a,s,t,\ldots$ have this property. More precisely, the expected convergence of P_L to a power law induces a Lee-Yang phenomenon for the corresponding cumulants generating function [Eq. (1)]. We show that this effect is related to the observed divergence of the moments. Furthermore, a scaling theory of the Lee-Yang zeros is proposed.

After some preliminaries (Sec. I), we give explicit analytical results (Sec. II) in several cases used as guidelines for subsequent analyses of a SOC model (Sec. III). We first study the truncated power law case where the cutoff tends to infinity when a parameter L (corresponding the lattice size in SOC models), tends to infinity (Sec. II A). We give in particular an analytic expression for the zeros. Then, we investigate the effect of a smooth cutoff (Sec. II B). We first discuss the properties that this cutoff must have, extrapolated from numerical simulations, and present some of the ansatz found in the literature (Sec. II B 1). We then explicitly compute the Lee-Yang zeros for a probability distribution obeying the finite-size scaling form proposed in [13] and converging to a power law as $L\to\infty$ (Sec. II B 2). We show, in particular, that when the power law exponent τ is larger than 1 there is a *violation* of the scaling usually observed in classical critical phenomena; namely, there is an anomalous logarithmic dependence on L for the angle that the zeros do with the real axis in the $t=\log(z)$ plane. We also show that when $\tau>1$ a bias is artificially induced by the numerical simulations, when the size of the sample used to generate the empirical probability distribution is fixed independently of the lattice size. This effect can be analyzed with the Lee-Yang zeros (Sec. II B 3). We then briefly study some other scaling form proposed in the literature and the effect of a finite size scaling violation on the Lee-Yang zeros (Sec. II B 4). Finally, in Sec. III, we present numerical simulations for the Lee-Yang zeros in the Zhang SOC model and compare them to the theoretical results obtained in Sec. II. We see no clearcut evidence of finite size scaling violation, but show that this model is quite sensitive to the numerical cutoff induced by a lattice size independent sampling. This can raise some doubts on the conclusions about scaling (finite size scaling, multifractal, or whatsoever) which can be drawn from some large lattice simulations done on this model in the literature.

I. PROBABILITY DISTRIBUTION AND LEE-YANG ZEROS

A. The finite size system

Let $P_L(n)=\mathrm{Prob}(N=n)$ be the probability distribution of the avalanche observable $N\in 1,\ldots,\xi_L$, where the index L refers to the characteristic size of the system. ξ_L, the maximal value that N takes is *finite*, whenever $L<\infty$, but diverges as $L\to\infty$. Therefore, the function

$$Z_L(z)=\sum_{n=1}^{\xi_L} z^n P_L(n), \tag{1}$$

where $z\in\mathbb{C}$, is a polynomial of degree ξ_L. In particular, since $Z_L(z)$ is an analytic function of z in the complex plane, all its moments exist. Denote by $E[\,]_L$ the expectation with respect to $P_L(n)$. Then we define

$$m_L(q)=\sum_{n=1}^{\xi_L} P_L(n)n^q \overset{\text{def}}{=} E[n^q]_L, \tag{2}$$

where q is a real (positive) number. For integer q, the $m_L(q)$'s are the moments of $P_L(n)$. Note that the normalization of $P_L(n)$ imposes $Z_L(1)=m_L(0)=1$.

For finite L, $Z_L(z)$ has ξ_L zeros in $\mathbb{C}$ that are either real $\leqslant 0$, or complex conjugate. Denote them by $z_L(k),k=1,\ldots,\xi_L$ and order them such that $0<|z_L(1)-1|\leqslant\cdots\leqslant|z_L(k)-1|\leqslant\cdots\leqslant|z_L(\xi_L)-1|$. Note that $z=0$ is a trivial zero, of multiplicity one, since $P_L(1)>0$. Write $z_L(k)=R_L(k)e^{i\theta_L(k)}=1+r_L(k)e^{i\nu_L(k)}$. Since all $P_L(n)$ are positive, $Z_L(z)$ has no zero on the positive real axis for finite L. Consequently, the logarithmic-generating function[1] $\log[Z_L(z)]$ is well defined on $\mathbb{R}_+^*$. Furthermore,

$$G_L(t)\overset{\text{def}}{=}\log[Z_L(e^t)] \tag{3}$$

is an analytic function of t. Define

[1]There is obviously a formal analogy between Eq. (1) [Eq. (3)] and a partition function (a free energy).

$$\chi_L(q)=\frac{d^q}{dz^q}\log[Z_L(z)]|_{z=1}, \tag{4}$$

where $z=e^t$. The quantities $\chi_L(q)$ are easily expressed in terms of the Lee-Yang zeros,

$$\chi_L(q)=(-1)^{q-1}(q-1)!\sum_{k=1}^{\xi_L}\frac{1}{(1-z_L(k))^q}. \tag{5}$$

B. The "thermodynamic" limit $L\to\infty$

1. Divergence of the moments and Lee-Yang phenomenon

As already written in the Introduction, a mathematical definition of the thermodynamic limit in SOC is a difficult task, beyond the scope of this paper. However, in [20] we developed a dynamical system approach for the Zhang model. Then, the thermodynamic formalism [21–24] can be used to define the finite size SOC state of a Gibbs measure[2] in this setting. It is then shown that the joint avalanche size distribution, for example, can be obtained in this formalism via a proper potential. The corresponding generating function for the time correlations, called the topological pressure, is the formal analog to the free energy. In this setting, it is argued that the critical behavior expected in the thermodynamic limit is manifested by a nonanalyticity of the topological pressure as $L\to\infty$, which can be linked to the loss of hyperbolicity characterizing the limit $L\to\infty$ of the Zhang model [25]. The loss of analyticity can be easily detected by looking at the generating function (1). Indeed, its zeros exhibit a Lee-Yang phenomenon.

The paper [20] is devoted to dynamical system aspects and to the mathematical foundation of a thermodynamic formalism for the Zhang SOC model, and the link between the scaling theory of Lee-Yang zeros in classical critical phenomena and the general SOC model is not addressed. This is the aim of the present paper. The results developed here are therefore complementary to [20] but are independent.

The present paper focuses on the analytic properties of the logarithmic-generating functions of the probability of avalanches indicators, when $L\to\infty$. It intends to analyze the variations in the Lee-Yang zeros properties if one uses the different scaling forms found in the SOC literature. Consequently, we collected the minimal implicit assumptions used in the SOC literature and we infer the consequences they lead to. This means that the result developed *a priori* holds for all SOC models.

It is first assumed that $P_L(n)$ converges to some probability distribution $P^*(n)$, $n=1,\ldots,\infty$. It is furthermore assumed that $P^*(n)$ has a power law tail,[3] namely $P^*(n)=K/n^\tau$, for a certain n range, $n=n_0,\ldots,\infty$, where $n_0<\infty,\forall L$. The number n_0 depends on the model and on the observable and introduces an extra parameter in the characteristics of the probability distribution. In the computations done in this paper there is no loss of generality is assuming that $n_0=1$. Therefore, in the sequel, $P^*(n)$ will stand for the power law K/n^τ, $n=1,\ldots,\infty$.

The measured exponent τ in SOC belongs to the interval $]1,2[$. $K=P^*(1)$ is the normalization constant. Consequently, $K=1/\zeta(\tau)$ where ζ is the Riemann ζ function.[4] Under the above assumptions, the moments $m_L(q)$ behaves asymptotically like $\Sigma_{n=1}^{+\infty}n^{q-\tau}$. This sum diverges for all $q>\tau-1$. It is numerically observed that $m_L(q)$ diverges like $m_L(q)\sim L^{\sigma(q)}$. A central issue is to compute the *scaling exponents* given by

$$\sigma(q)\overset{\text{def}}{=}\lim_{L\to\infty}\frac{\log[m_L(q)]}{\log(L)}=\lim_{L\to\infty}\frac{\log[\chi_L(q)]}{\log(L)}. \tag{6}$$

$\sigma(q)$ is an nondecreasing function. Its Legendre transform is found under the name of ''multifractal spectrum'' in the SOC literature [14] though it has no direct connection with the fractal geometry of the invariant set.

Since $P^*(n)$ is a probability distribution the limiting generating function

$$Z^*(z)=\lim_{L\to\infty}Z_L(z)=\sum_{n=1}^{\infty}P^*(n)z^n \tag{7}$$

is still an analytic function in the open unit disc in $\mathbb{C}$. However, the logarithmic-generating function of $P^*(n)$ is not analytic near to $z=1$ since the derivative of order $q>\tau-1>0$ diverge. The corresponding singularity is related to the behavior of the zeros in the vicinity of $z=1$. More precisely, fix $\epsilon>0$ arbitrary small, call $I_L(\epsilon)=\{i||z_L(i)-1|<\epsilon\}$ and $n_L(\epsilon)=\#I_L(\epsilon)$, where # denotes the cardinality of a set. Then the divergence of $\chi_L(q)$ is governed by the zeros which accumulate in $I_L(\epsilon)$. Namely, the sum (5) contains a singular term

$$\gamma_s(L,\epsilon,q)=(-1)^{q-1}2(q-1)!\sum_{k=1}^{n_L(\epsilon)/2}\frac{\cos[q\nu_L(k)]}{r_L^q(k)} \tag{8}$$

which diverges as $L\to\infty$, while the remaining part in the sum is regular and is bounded by $(q-1)!/\epsilon^q$ as $L\to\infty$.

2. Scaling of the zeros in classical critical phenomena

In the theory of classical critical phenomena, it is possible to relate the scaling exponents of quantities such as magnetization or latent heat, susceptibility, etc. . . . to the behavior of the Lee-Yang zeros near to $z=1$. There exists a scaling theory based on earlier works by Lee and Yang [17], Grossmann and Rosenhauer [26], Abe [27], Suzuki [28], Privman and Fisher [29], Itzykson *et al.* [30], and Glasser *et al.* [31].

[2]The particular structure of the Zhang model allows us to symbolically encode the dynamics. In the framework of the thermodynamic formalism a Gibbs measure is a probability measure weighting the symbolic chains encoding the trajectories with an exponential weight called a potential (see [20] for details).

[3]Note that the limiting probability distribution is defined only if $\tau>1$.

[4]In general the normalization constant depends on n_0.

Many analytical and rigorous results are also known (for example [32–35]). A lot of efforts have been devoted to the study of ferromagnetic systems (e.g., Ising or Potts models) though many other examples have also been studied in the literature. In this setting, one distinguishes the zeros in the complex magnetic field (called Lee-Yang zeros) from the zeros in the temperature plane (Fisher zeros). In the first case, the zeros lie on the unit circle for a large class of models including the Ising's one.

The Fisher zeros usually approach $t=0$ in the $t=\log(z)$-complex plane with a constant angle ϕ (this is the case for the Ising model and mean-field ferromagnetic models [31]). This allows us to obtain simple scaling expression for the singular part of the free energy $f^s(t)$, where t is the reduced temperature. In this setting an analytic expression for $f^s(t)$ has been obtained by Grossmann and Rosenhauer [26], and, later on, extended by Itzykson *et al.* [30] by using the renormalization group theory. This approach has been extended by Glasser *et al.* [31] to mean-field models. In the thermodynamic limit $f_s^{\pm}\sim A_{\pm}|t|^{2-\alpha}$, where $A_{\pm}$ are universal constants ($\pm$ label the two magnetic phases at low temperature) and α is the critical exponent for the specific heat. It follows from the renormalization group analysis [29] that the singular part of the free energy obeys a finite-size scaling form:

$$f^s(t,V)=\frac{1}{V}\mathcal{F}[t(AV)^{1/(2-\alpha)}], \tag{9}$$

where V is the finite volume and $\mathcal{F}$ a universal function. Accordingly, the n first Fisher zeros are given by

$$t_V(n)=\left[\frac{2\pi}{[A_+^2+A_-^2-A_+A_-\cos(\pi\alpha)]}\frac{n}{V}\right]^{1/(2-\alpha)}e^{i(\pi-\phi)}. \tag{10}$$

The angle ϕ is related to $A_{\pm},\alpha$ by

$$\tan[(2-\alpha)\phi]=\frac{\left[\cos(\pi\alpha)-\dfrac{A_-}{A_+}\right]}{\sin(\pi\alpha)}.$$

This situation, where the zeros approach the singularity with a *constant angle* ϕ and where the modulus scales like the volume to a certain power will be referred to as *normal scaling* in the sequel.

It seems a general observation [26] that the zeros lie on a curve or a union of curves dividing the complex plane in different regions of analyticity of $Z^*(z)$, corresponding to different phases. More precisely, it has been recently proved by Biskup *et al.* [34] that the zeros lie on curves with a simple analytic expression and accumulate in the thermodynamic limit on loci where the various branches of the free energy have the same modulus. This last result suggests that a wide extension of the Lee-Yang phenomena can be made toward dynamical systems near to a critical point. We now develop this aspect for the analysis of the logarithmic-generating function of probability distribution in the SOC framework. In the sequel, we will not distinguish between the Lee-Yang zeros and the Fisher zeros and we will use the generic terminology "Lee-Yang" for the zeros.

II. SCALING THEORY OF SOC AND LEE-YANG ZEROS

In this section we establish analytical results for various finite size scaling forms found in the SOC literature. These results are then used in Sec. III for the analysis of the empirical data obtained from a numerical simulation of a SOC model. As a matter of fact, for finite size SOC systems, the power law is truncated by a cutoff characterized by a length scale Λ_L, usually different from ξ_L. The starting point is therefore the analysis of a truncated power law with a sharp cutoff at a value Λ_L. This is a useful example for subsequent analysis since the analytic form of $P_L(n)$ and the cutoff is known.

A. Zeros of a truncated power law

Assume that $P_L(n)=C_L/n^{\tau}, n=1,\ldots,\xi_L$, where C_L is a normalization constant and $\xi_L=\Lambda_L=L^{\beta}, \tau>1, \beta>0$. Furthermore, assume that $\tau<2$.

1. Scaling of the moments and logarithmic-generating function

For $0\leqslant q\leqslant \tau-1$, $m_L(q)\to\zeta(\tau-q)/\zeta(\tau)$ and consequently $\sigma(q)=0$. The nonzero scaling exponents $\sigma(q)$ can be obtained from the following integral approximation of $m_L(q)$, which becomes exact in the limit $L\to\infty$, provided $q\geqslant\tau-1$,

$$m_L(q)\sim C_L\Lambda_L^{q+1-\tau}\int_{1/\Lambda_L}^{1}u^{q-\tau}du=\frac{C_L}{q+1-\tau}(\Lambda_L^{q+1-\tau}-1). \tag{11}$$

Then, $\sigma(q)=\beta(q+1-\tau)$ for (real) $q>\tau-1$. Note, however, that for finite size, one has additional L-dependent terms which have to be considered when extrapolating from numerical simulations. It is also interesting to note that formula (11) gives useful information on the *rate of convergence* of $m_L(q)$ to a constant for $q<\tau-1$. Indeed, the convergence is *not uniform* in q, namely the *closer* is q to $\tau-1$ the *slower* is the convergence rate. This means that a *systematic bias due to finite size* is introduced in the numerical simulations when dealing with the q's close to $\tau-1$. This produces a spurious curvature, near to $\tau-1$, for the function $\sigma(q)$ extrapolated from numerical data. This effect, which disappears as $L\to\infty$, can lead to a misleading conclusion since it can be interpreted as an evidence of a multifractal scaling.

The scaling exponents can also be obtained from the scaling of the logarithmic-generating function. Indeed, the generating function writes

$$Z_L(t)=1+\sum_{n=1}^{\xi_L}P_L(n)(e^{tn}-1)\sim 1+C_L\Lambda_L^{1-\tau}\int_{1/\Lambda_L}^{1}u^{-\tau}(e^{t\Lambda_L u}-1)du. \tag{12}$$

Set $t'=\Lambda_L t$ and

$$\psi(t')\overset{\text{def}}{=}\int_0^1 u^{-\tau}(e^{t'u}-1)du=\sum_{n=1}^{\infty}\frac{t'^n}{n!}\int_0^1 u^{n-\tau}du$$
$$=\sum_{n=1}^{\infty}\frac{t'^n}{n!(n+1-\tau)}. \quad (13)$$

Note that since $\tau<2$, this integral is finite as can easily be checked by integration by part. Therefore the commutation of the integral and the series is allowed.

Consequently,

$$Z_L(t)\sim 1+C_L\Lambda_L^{1-\tau}\psi(t')=1+C_L L^{\beta(1-\tau)}\psi(tL^{\beta}) \quad (14)$$

and

$$G_L(t)=\log[1+C_L L^{\beta(1-\tau)}\psi(tL^{\beta})]. \quad (15)$$

$\psi(t)$ is a smooth function of t which vanishes as $t\to 0$. Therefore, for $t\to 0$

$$G_L(t)\sim C_L L^{\beta(1-\tau)}\psi(tL^{\beta}), \quad (16)$$

which gives the right scaling for the moments by differentiating with respect to t at $t=0$. One remarks that this scaling form is analogous to the form (9).

2. Lee-Yang zeros

From Eq. (14) the zeros are approximately given by

$$\psi(t')=-C_L\Lambda_L^{\tau-1}=-C_L L^{\beta(\tau-1)}. \quad (17)$$

Since $\tau>1$, $\Lambda_L^{\tau-1}$ diverges. $\psi(t')$ is an increasing function of the real variable t' which vanishes as $t'=0$ and tends to $-\infty$ when $t'\to-\infty$. Furthermore, for any $K>0$, $\psi(t')$ is bounded by $\psi(K)$ in the ball $|t'|<K$ in the complex plane. Consequently, Eq. (17) can be fulfilled only if $t'_L(k)$'s have *a diverging modulus as L* grows. On the other hand, since $t_L(k)=t'_L(k)/\Lambda_L$ converges to zero, $|t'_L(k)|$ must grow slower than Λ_L. It grows in fact like $\log(\Lambda_L)$ as shown below.

Note that, conversely, when $\tau<1$, $-C_L L^{\beta(\tau-1)}$ goes to zero in the thermodynamic limit.[5] Then, the zeros are formally given by

$$t_L(k)=\frac{1}{\Lambda_L}\psi_k^{-1}(-C_L\Lambda_L^{\tau-1})\sim\frac{1}{\Lambda_L}\psi_k^{-1}(0),$$

where ψ_k^{-1} is the kth branch of the inverse of ψ in the complex plane. Consequently, the zeros have a simple scaling in these case similar to Eq. (10). In particular, *the argument does not depend on L*.

The observed values of the critical exponents in SOC, $\tau>1$, induces anomalous scaling that can be observed on the Lee-Yang zeros. Though the form (14) can be used to compute the Lee-Yang zeros, it is easier to use

$$Z_L(t)=\sum_{n=1}^{\Lambda_L}P_L(n)e^{tn}\sim C_L\Lambda_L^{1-\tau}\int_{1/\Lambda_L}^1 h(u,t')du, \quad (18)$$

where $h(u,t')=u^{-\tau}e^{t'u}$. There exists several techniques to compute the Lee-Yang zeros in statistical mechanics. A standard way is to argue that the asymptotic free energy admits different analytic continuation in different regions of the complex plane, separated by Stokes lines where the zeros accumulate in the thermodynamic limit. Indeed, because of the large number of terms in the polynomial which make up the partition function, the behavior tends to become dominated by some set of the coefficients. Thus we have different analytic functions in different regions of the complex plane. These functions have oscillating phases but smoothly varying amplitude. The zeros locate then on Stokes boundaries where two types of behavior have comparable magnitude [30,31,34]. The Stokes boundaries become cuts in the thermodynamic limit. Across the boundaries the free energy has a regular real part and jumps in the imaginary part [26].

Applying this strategy to our formal partition function (18), one identifies easily two regions. For real t', as u grows from to 0 to ∞, $h(u,t')$ first decay like $u^{-\tau}$ until a minimum $u_-=\tau/t'$. Therefore, $u_->1/\Lambda_L$ when $t<\tau$. For $u>u_-$, $h(u,t')$ grows exponentially like $e^{t'u}$. Therefore, when t' is small the integral in Eq. (18) is essentially dominated by the algebraic decay $u^{-\tau}$ and $\int_{1/\Lambda_L}^1 h(u,t')du\sim[1/(\tau-1)][\Lambda_L^{\tau-1}-1]$. On the other hand, for large t', $u_-\to 0$ and the algebraic part is negligible compared to the exponential part. Hence $\int_{1/\Lambda_L}^1 h(u,t')du\sim\int_{u_-}^1 e^{t'u}du=(1/t')[e^{t'}-e^{\tau}]$. This argumentation extends to complex t' and suggests that one can roughly divide the t complex plane into two regions where $Z_L(t)$ has a different analytic form: for sufficiently small t' the algebraic part dominates, while for large t' the exponential part is dominant. Then the zeros have to stay at the place where the two forms are of the same order. Therefore an approximate equation for the location of the zeros is given by

$$\frac{1}{t'}[e^{t'}+a_1t'-a_2]=-\frac{\Lambda_L^{\tau-1}}{\tau-1}, \quad (19)$$

where $a_1=1/(1-\tau), a_2=e^{\tau}$.

The solutions of $e^{t'}/t'=-\Lambda_L^{\tau-1}/(\tau-1)$ are given by

$$t'_L(k)=\Lambda_L t_L(k)=-W_k\left(\frac{\tau-1}{\Lambda_L^{\tau-1}}\right), \quad (20)$$

where $W_k(x)$ is the kth branch of the Lambert function [36]. Note that the Lambert function has infinitely many branches and consequently the equation $e^{t'}/t'=-\Lambda_L^{\tau-1}/(\tau-1)$ has infinitely many solutions. Indeed, in replacing the initial sum by an integral in Eq. (18) we have introduced spurious zeros which have to be removed for finite L. In the sum (18) one

[5]Though the limit probability is not defined it is nevertheless possible to investigate the finite size scaling properties for the zeros of the finite size generating function.

has a step of integration $1/\Lambda_L$ which defines a lower cutoff in the scales one has to consider. Consequently, only the branches $k=-\Lambda/2 \ldots \Lambda/2$, where one takes into account the symmetry of the zeros with respect to the real axis, are relevant.

The Lambert function W_k admits the following expansion, for large $|\log(x)|$ [36]:

$$W_k(x)=\log_k(x)-\log[\log_k(x)]$$

$$+\sum_{l\geqslant 0}\sum_{m\geqslant 1} c_{lm}\frac{[\log\log_k(x)]^m}{(\log_k x)^{l+m}}, \qquad (21)$$

where $\log_k$ is the kth branch of the complex logarithm and $c_{lm}=(1/m!)(-1)^l\left[{l+m \atop l+1}\right]$ is expressed in terms of the Stirling numbers of the first kind $(-1)^{m+n}\left[{n \atop m}\right]$ [36].

The double series $\Sigma_{l\geqslant 0}\Sigma_{m\geqslant 1}c_{lm}\{[\log\log_k(x)]^m/(\log_k x)^{l+m}\}$ is absolutely convergent for sufficiently large $|\log(x)|$ [36]. Since we are only interested in the asymptotic divergence when L grows, one can therefore neglect the series in the asymptotic. Note, however, that the convergence to the asymptotic regime where the series becomes negligible *is faster when the product* $\beta(\tau-1)$ *is larger*.

The term $\log\{\log_k[\Lambda^{\tau-1}/(\tau-1)]\}$ cannot be neglected compared to $\log_k[\Lambda_L^{\tau-1}/(\tau-1)]$ since it contains crucial k dependence for the real part of $t_L(k)$ (see below). It is interesting to note that it introduces a $\log(\log L)$ finite size scaling correction. A similar correction as been found in [37] for the Potts model with $q\geqslant 4$.

The corrections due to the other terms of Eq. (19) become rapidly negligible as can easily be seen by a perturbation expansion.

One finally obtains the following asymptotic form for the Lee-Yang zeros of the truncated power law:

$$\mathrm{Re}[t_L(k)]\sim\frac{-\log\left(\frac{\tau-1}{\Lambda_L^{\tau-1}}\right)+\frac{1}{2}\log\left[\log^2\left(\frac{\tau-1}{\Lambda_L^{\tau-1}}\right)+4k^2\pi^2\right]}{\Lambda_L}, \qquad (22)$$

$$\mathrm{Im}[t_L(k)]\sim\frac{2k\pi}{\Lambda_L}-\frac{1}{\Lambda_L}\arctan\left(\frac{2\pi k}{\log\left(\frac{\tau-1}{\Lambda_L^{\tau-1}}\right)}\right). \qquad (23)$$

The term $\log\{\log_k[(\tau-1)/\Lambda_L^{\tau-1}]\}$ introduces a k dependence which implies in particular that the zeros (in the z plane) do not lie on circle but on a more complicated curve (see Fig. 1). This dependence remains important, even for the first zeros, up, to very large L, especially if τ is close to 1. Indeed, for a fixed k the term $\log^2[(\tau-1)/\Lambda_L^{\tau-1}]$ dominates the term $4k^2\pi^2$ only for $L\gg[(\tau-1)e^{2\pi k}]^{1/\beta(\tau-1)}$ (say, for $\tau=1.25,\beta=2.67$ this corresponds to a $L\gg 1500$).

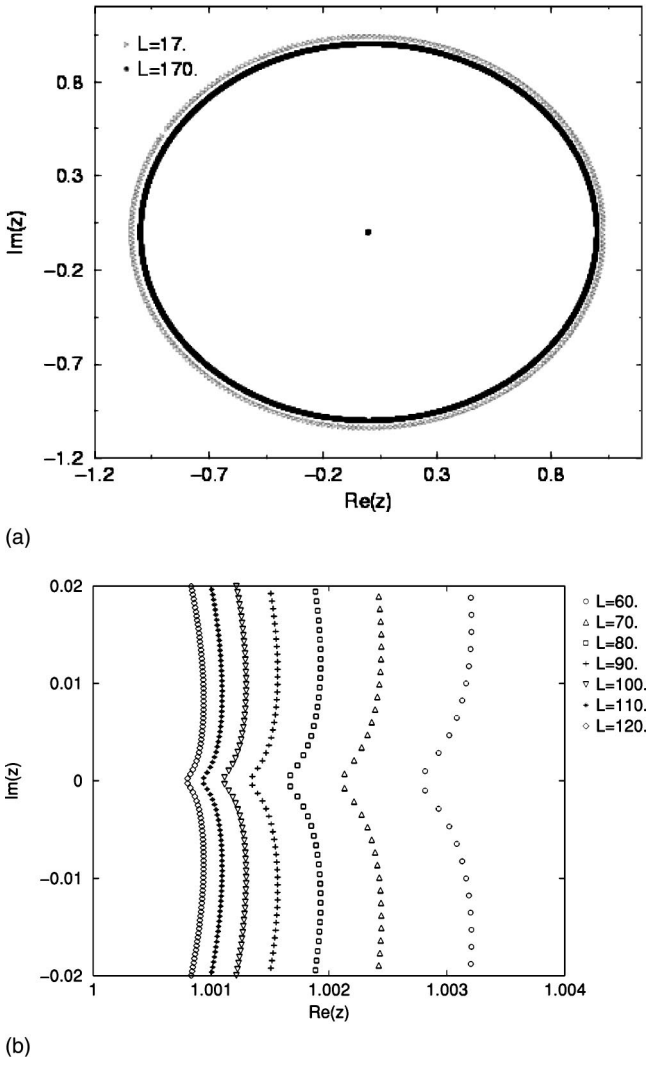

FIG. 1. (a) Lee-Yang zeros for various L values in the z complex plane $\beta=2,\tau=1.9$. (b) Local behavior near to $z=1$.

The arctan term in the imaginary part acts essentially as a phase term $-(1/\Lambda_L)\arctan\{2\pi k/\log[(\tau-1)/\Lambda_L^{\tau-1}]\}$ which is slowly varying (in the k variable) compared to the dominant term $2k\pi/\Lambda_L$. Furthermore, since the arctan is bounded above by $\pi/2$ it is rapidly negligible as k grows. Therefore, one can consider with a good approximation that $\mathrm{Im}[t_L(k)]\sim 2k\pi/\Lambda_L$.

The argument of $t_L(k)$ formally corresponds to the angle that the Fisher zeros do with the real axis in critical phenomena. For a power law with $\tau<1$ this angle is independent of L as discussed above. Conversely, for $\tau>1$ it is given by

$$\arg[t_L(k)] \sim \arctan\left(\frac{2k\pi}{-\log\left(\frac{\tau-1}{\Lambda_L^{\tau-1}}\right) + \frac{1}{2}\log\left[\log^2\left(\frac{\tau-1}{\Lambda_L^{\tau-1}}\right) + 4k^2\pi^2\right]} \right). \tag{24}$$

One observes therefore a *logarithmic deviation to the normal scaling on the argument of the* $t_L(k)$*'s*. The conclusion is therefore that, though the truncated power law obeys the classical *finite size scaling* form (9), the Lee-Yang zeros display nevertheless an *anomalous scaling* due to the exponent $\tau > 1$ (see Fig. 2).

In the z plane the zeros $z_L(k) = e^{t_L(k)}$ are approximately given by

$$R_L(k) = |z_L(k)| \sim 1 + \mathrm{Re}[t_L(k)], \tag{25}$$

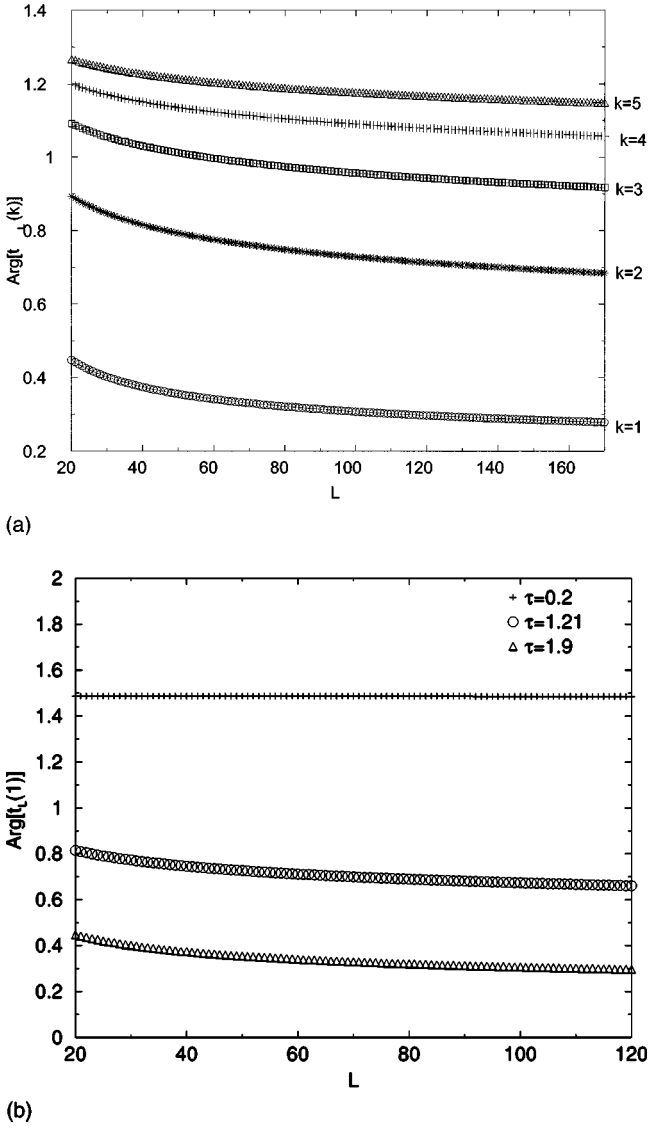

FIG. 2. (a) Argument of the Lee-Yang zeros in the t complex plane versus L for various k values, $\beta = 2, \tau = 1.9$. (b) Normal ($\tau = 0.2$) and anomalous ($\tau = 1.21, \tau = 1.9$) scaling of the angle with the real axis for various τ value.

$$\theta_L(k) = \mathrm{Im}[t_L(k)] \sim \frac{2k\pi}{\Lambda_L} = \frac{2k\pi}{L^\beta}. \tag{26}$$

Therefore the arguments $\theta_L(k)$ of the zeros in the z complex plane are uniformly distributed in $[-\pi, \pi]$ with a good approximation [Fig. 3(b)].

Finally, one can determine the exponents τ, β from the Lee-Yang zeros. The exponent β corresponds to the scaling exponent of the correlation length ξ_L. Eq. (26) provides *a straightforward way* to compute it. Furthermore, the exponent τ can be obtained from Eq. (22). The term $4\pi^2 k^2$ certainly rapidly dominates the term $\log^2[(\tau-1)/\Lambda_L^{\tau-1}]$ in the modulus $R_L(k)$ as k grows. This is *a fortiori* true for $k \sim \Lambda_L$ which corresponds to the zeros the farthest from $z = 1$. Consequently,

$$R_L(\theta) \sim \left[\frac{\Lambda_L^{\tau-1}}{\tau-1} \sqrt{\log^2\left(\frac{\tau-1}{\Lambda_L^{\tau-1}}\right) + 4\theta^2\Lambda_L^2} \right]^{1/\Lambda_L} \sim \left[\frac{2\theta\Lambda_L^\tau}{\tau-1} \right]^{1/\Lambda_L}. \tag{27}$$

If one takes $k = \Lambda_L/2$ (corresponding to an angle π), one has

$$\tau = \lim_{L\to\infty} \frac{\Lambda_L \log[R_L(\pi)]}{\log(\Lambda_L)}, \tag{28}$$

which allows a possible determination of τ from the scaling of the Lee-Yang zeros [Fig. 4(b)]. Note, however, that the convergence is logarithmic in L.

3. Numerical checks

Since it is easy to generate numerically a power law distribution one is *a priori* free to choose any values for τ and β. However, the closer τ is to 1 the slower is the convergence to the asymptotic regime where the formulas obtained in the previous section hold. More precisely, the rate of convergence is essentially governed by the product $\beta(\tau-1)$. The closer is τ to 1 the larger has to be β. But the larger β, the faster the degree of the polynomial increases with L and therefore the time needed for the computation of the zeros increase. On the other hand, since the theory developed here is independent of the actual value of β, τ (provided $\tau > 1$), we mainly studied examples where $\beta = 2$ and $\beta = 2.2$ which gives a reasonable increase in the polynom degree, and $\tau = 1.9$ such that the product $\beta(\tau-1) \sim 2$.

We first depicted the pattern of zeros, for different sizes, in Fig. 1. One notices the slow convergence to the unit circle, and the shape of the curve near to $z = 1$: this is not a circle.

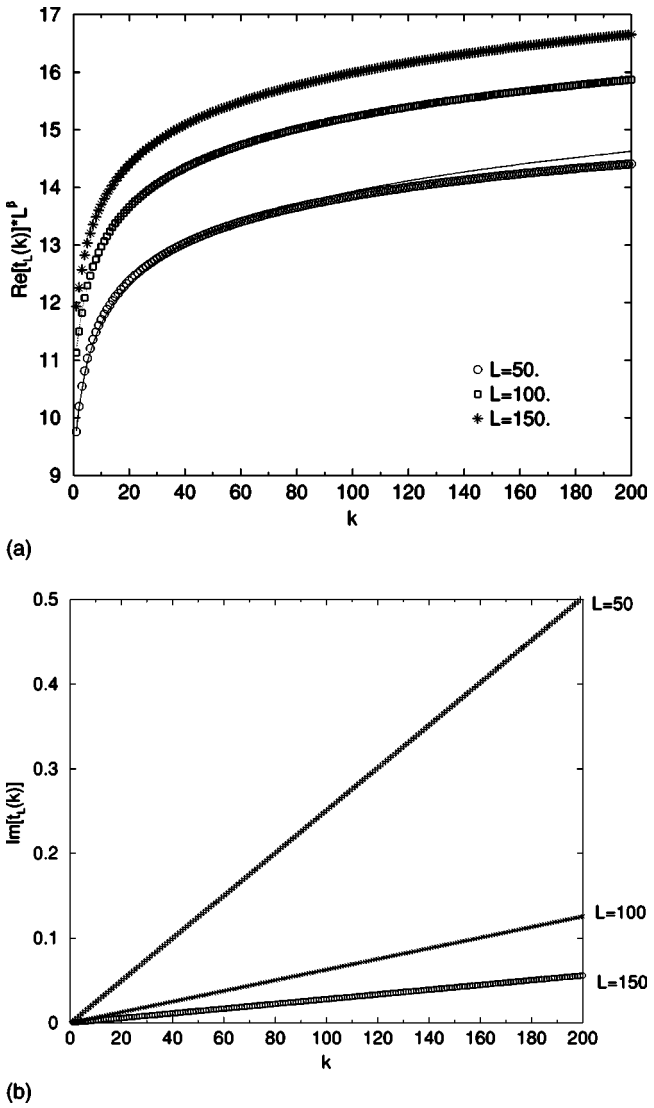

FIG. 3. Lee-Yang zeros in the t complex plane, versus k for various L values. (a) Real part multiplied by Λ_L. (b) Imaginary part.

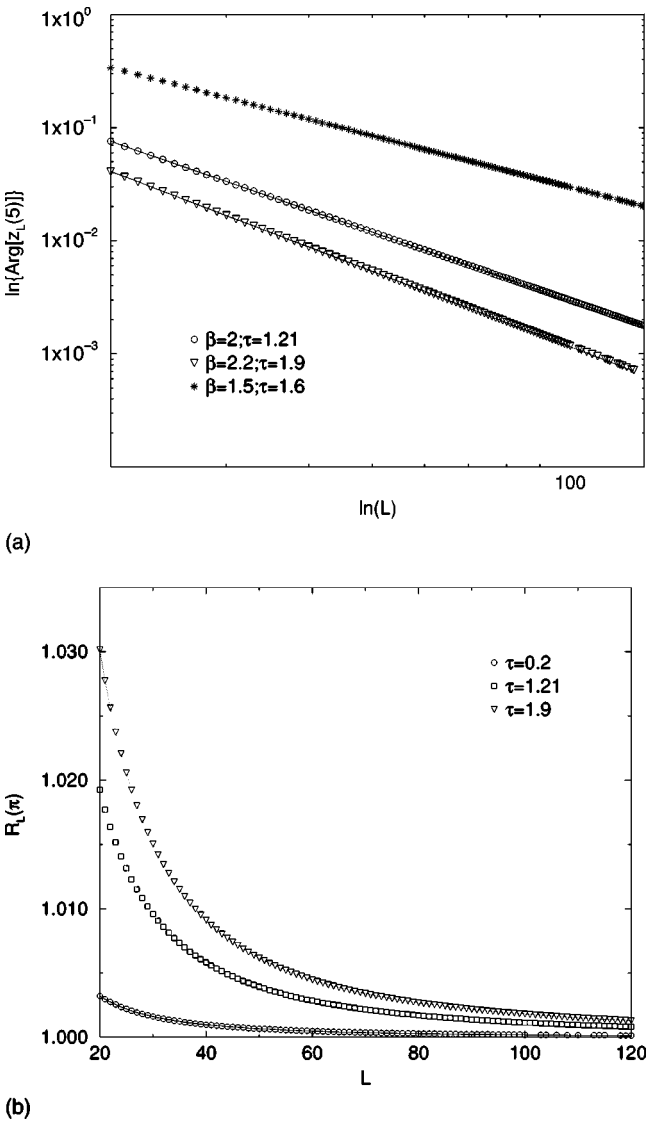

FIG. 4. (a) Argument of the fifth Lee-Yang zero in the z complex plane, versus L for various β values. (b) $R_L(\pi)$ as a function of L for various τ values. The fitting curves are plotted using lines.

We plotted Fig. 3 the real and imaginary part of the zeros in the t plane. For the real part we tried a fit of the form $r(k)=\{-\log(a)+\frac{1}{2}\log[\log^2(a)+4\pi^2k^2]\}/\Lambda_L$ where a is a free parameter. The formula (22) gives $a_{th}=(\tau-1)/\Lambda_L^{\tau-1}$ but, in the several approximations we made, we neglected some constants, and one expects a to be different from the theoretical value, with an error that should decrease as L grows. The result of the fitting is represented Fig. 3(a) for the 200 first zeros. We found indeed that the experimental value a_{exp} is closer and closer to its theoretical value as L increases and that our approximation is better and better as L increases. For $L=50$, $a_{th}=7.87\times10^{-4}, a_{exp}=5.6\times10^{-4}\pm4\times10^{-5}$; for $L=100$, $a_{th}=2.26\times10^{-4}, a_{exp}=1.5\times10^{-4}\pm3\times10^{-5}$ and for $L=150$, $a_{th}=1.09\times10^{-4}, a_{exp}=7.1\times10^{-5}\pm810^{-7}$. The imaginary part is plotted in Fig. 3(b) together with the theoretical prediction $\mathrm{Im}[t_L(k)]=2\pi k/L^{\beta}$ (straight lines). We noted a slight deviation of the first zeros to $2\pi/\Lambda_L$ due to the correction term in Eq. (26).

In Fig. 2(a) we plotted the argument of $t_L(k)$ as a function of L for $k=1,\ldots,5$. We notice the logarithmic deviation to the normal scaling as predicted by formula (24). We tried to fit these curves with a fit of the form $\arctan(2k\pi/\alpha[\log(x)+\gamma]+\frac{1}{2}\log\{\alpha^2[\log(x)+\gamma]^2+4k^2\pi^2\})$, where α,γ are free parameters. In Fig. 2(b) we show the different scaling occurring for $\tau<1$ (normal scaling) or $\tau>1$ (anomalous scaling).

Finally we argued above that the exponents β and τ can be determined with a good accuracy from the scaling of the zeros. In Fig. 4(a) we plotted $\arg[z_L(5)]=\theta_L(5)$ as function of L for $\beta=1.5,\tau=1.6;\beta=2,\tau=1.21;\beta=2.2,\tau=1.9$, and $L=20,\ldots,120$. We choose the fifth zeros rather than the first ones since for the first zeros the correction coming from the arctan term in Eq. (23) influences slightly the scaling for small L. We tried a fit of the form C/x^{β} where $C_{th}\sim10\pi=31.415\ldots$. The fits shown on the figure gave, respectively, $\beta=1.507\pm0.002;\beta=2.007\pm9\times10^{-3};\beta=2.205\pm\times0.001$.

For the determination of τ we used Eq. (27) for $\tau=0.2$, 1.21, 1.9, and $\beta=2$. We have interpolated the data with a fit form $e^{\beta\tau\log(ax)/x^{\beta}}$ where a,τ were free parameters. For $L=20,\ldots,120$, we found, respectively, $0.1998(2)\pm6.10^{-6}$, $1.207(5)\pm7.10^{-5}$, and $1.89(5)\pm0.0001$ for the value of τ. This is satisfactory especially when taking into account the smallness of the L's we considered.

B. General case: the structure of the cutoff

The observed probability distribution of avalanches observables in SOC models is in general a powerlaw truncated by a cutoff function associated with finite-size effects. Except for a few cases [38], the analytic form of the cutoff is not known. Consequently, various scaling forms have been proposed in the SOC literature. In this section we grasp the most common scaling forms and discuss their effect on the Lee-Yang zeros. We also investigate the effect of the sampling cutoff inherent to numerical simulations.

1. General assumptions about the cutoff function

Since $P_L(n)$ is expected to converge to a power law $Kn^{-\tau}$ one can write, without loss of generality, the finite size probability under the form

$$P_L(n)=\frac{C_L}{n^{\tau}}f_L(n),\ 1\leqslant n\leqslant\xi_L \tag{29}$$

where C_L is a normalization constant depending on L. $f_L(n)$ is the finite size cutoff.

The graph obtained from numerical simulations suggests that $f_L(n)$ is a regular function which obeys

$$\text{(i)}\ \lim_{L\to\infty}f_L(n)=1,\ \ \forall n\leqslant\xi_L,$$

$$\text{(ii)}\ \forall p>0,\ \ \lim_{n\to\infty}n^{p}f_L(n)=0,\ \forall L.$$

The property (i) corresponds to the pointwise convergence to a power law. (ii) characterizes the observed fact that the tail of $P_L(n)$ decreases faster than any power of n (e.g., is least exponentially decreasing).

These properties are not sufficient for a scaling theory and further assumptions have to be made. We now discuss various scaling forms that one can find in the literature and also the numerically induced cutoff effects.

Finite-size scaling. In 1990, Kadanoff *et al.* [13] proposed a finite-size scaling ansatz where

$$f_L(n)=g\left(\frac{n}{\Lambda_L}\right), \tag{30}$$

g being a universal function. $\Lambda_L=L^{\beta}$ is the characteristic scale for a lattice of size L and $\xi_L=\alpha\Lambda_L$ where α is a constant. The case of a truncated power law developed in Sec. II A corresponds to the particular case where $\alpha=1$, and $g(x)$ is equal to 1 for $x\in[0,1]$ and zero otherwise. Note that in this case the property (ii) has the consequence that

$$\text{(iii)}\ \lim_{x\to0}g(x)=1.$$

Multifractal scaling. In the same paper, Kadanoff *et al.* [13] discussed another form of scaling, that is

$$\frac{\log[P_L(n)]}{\log\left(\frac{L}{L_0}\right)}=f\left(\frac{\log\left(\frac{n}{n_0}\right)}{\log\left(\frac{L}{L_0}\right)}\right), \tag{31}$$

where f is universal and does not depend explicitly on L. L_0,n_0 are some constants that can be omitted by a suitable redefinition of the quantities, then

$$P_L(n)=L^{f(\log n/\log L)}. \tag{32}$$

This representation is called by the authors an $f-\alpha$ representation, α being the quantity $\log(n/n_0)/\log(L/L_0)$. In this case one has a whole spectrum of scaling indices, i.e., all the values taken on by $df/d\alpha$. In the general case f is nonlinear. Then the universality class is given by the function f, rather than by a finite set of critical exponents. In this case, the scaling exponents are nonlinear functions of q.

Finite size scaling violation and convergence to a power law. Another scaling form has been introduced by Lise and Paczuski [16] from numerical simulations on the Olami-Feder-Christensen model.[6] Lise and Paczuski analyzed their data with the following form for $P_L(n)$:

$$P_L(n)=C_Ln^{-\tau}L^{F_L(\log(n)/\log(L))},\quad n=1,\ldots,L^{\beta_L} \tag{33}$$

where β_L is now L dependent, $\beta_L<\beta<\infty$ and $\beta_L\to\beta$ as $L\to\infty$. Furthermore, the numerical plot of $F_L(x)$ in [16] suggests that $F_L(x)$ converges to a "step" function $Y(x-\beta)$ as $L\to\infty$, where $Y(u)=0,\ u\in]-\infty,0[$, $Y(0)=C$ and $Y(u)=-\infty,\ u\in]0,\infty]$. The finite size scaling case corresponds to $F_L(x)=\log[g(L^{x-\beta})]/\log L$ where g is defined in Eq. (30). This example is quite interesting since it gives an example of a probability distribution violating Eq. (30) but converging nevertheless to a power law (namely the exponents τ and β are still meaningful). We remark indeed that the corresponding probability distribution is *not multifractal* in the sense of [14] since it is easy to check that the scaling exponents are given by $\sigma(q)=\beta(q+1-\tau),\ \forall q\geqslant\tau-1$ and $\sigma(q)=0,\forall q<\tau-1$. This case is therefore intermediate between the finite-size scaling (30) and the multifractal case (32). In the following sections we discuss the behavior of the Lee-Yang zeros in these different cases.

2. Finite-size scaling

We show in this section that the behavior of the Lee-Yang zeros in the finite size scaling case is essentially the same as for the truncated power law, provided g in Eq. (30) fulfills the conditions (i),(ii),(iii) in the previous section.

[6] B.C. is very grateful to M. Paczuski for illuminating discussions on this topic in Bielefeld.

It is well known that the moments obey the same scaling. This can be recovered from the generating function (1). Provided $\tau<2$ it scales as $L\to\infty$ like

$$Z_L(t)\sim 1+C_L\Lambda_L^{1-\tau}[\Upsilon_\alpha(t')-\Upsilon_{1/\Lambda_L}(t')]\sim 1 + C_L\Lambda_L^{1-\tau}\Upsilon_\alpha(t')+C_L\psi(t)\sim 1+C_L\Lambda_L^{1-\tau}\Upsilon_\alpha(t') \tag{34}$$

for $t\to 0$ in the t complex plane. In this equation $t'=\Lambda_L t$ and

$$\Upsilon_\gamma(t')\overset{\text{def}}{=}\int_0^\gamma u^{-\tau}g(u)(e^{t'u}-1)du=\sum_{n=1}^{\infty}\frac{t'^n}{n!}\int_0^\gamma u^{n-\tau}g(u)du. \tag{35}$$

Consequently, near to $t=0$, $Z_L(t)\sim 1+C_L L^{\beta(1-\tau)}\Upsilon_\alpha(tL^\beta)$ and $G_L(t)\sim C_L L^{\beta(1-\tau)}\Upsilon_\alpha(tL^\beta)$. As expected one obtains the same scaling as for a truncated power law. The only change is that the function Υ depends now on the g function.

The zeros of $Z_L(t)$ are therefore well approximated by

$$\Upsilon_\alpha(t')\sim -C_L\Lambda_L^{\tau-1} \tag{36}$$

which is completely analogous to Eq. (17). Therefore, the same conclusions hold: Eq. (36) can be fulfilled only if the solutions $t'_L(k)$ have a diverging modulus as L grows. The computation of the zeros is essentially the same as in Sec. II A with slight complications due to the presence of the function g.

One can write

$$Z_L(t)\sim C_L\Lambda_L^{1-\tau}\int_{1/\Lambda_L}^{\alpha}h(u,t')du, \tag{37}$$

where now $h(u,t')=u^{-\tau}g(u)e^{t'u}$. Recall that, by hypothesis, $g(u)$ is an at least exponentially decreasing function. As u grows from to 0 to ∞, $h(u,t')$ first decay like $u^{-\tau}$ until a minimum u_- after which $h(u,t')$ grows exponentially like $e^{t'u}$. u_- tends to 0 as $t'\to\infty$. More precisely, if t' is sufficiently large, from (iii) $g(u)$ is essentially 1 on the interval $[0,u_-]$ and therefore u_- is approximately given by $t'u_-^{-\tau}=\tau u_-^{-\tau-1}$. Consequently $u_-\sim\tau/t'$. When u is sufficiently large the decay coming from $g(u)$ compensates the exponential increase of $e^{t'u}$. Therefore, there is a maximum u_+ after which $h(u,t')$ tends to zero with a rate given by $g(u)$. Here, $h(u,t')$ is essentially $g(u)e^{t'u}$. Therefore u_+ is given by $t'g(u_+)+g'(u_+)=0$ or $t'=-d\log[g(u_+)]/du$, where $-d\log[g(u)]/du$ is a function which increases faster than u by (ii). Consequently, u_+ diverges as $t'\to\infty$. Since α is bounded by assumption, $u_+>\alpha$ for t' (L) sufficiently large. But, from Eq. (36) we know that the modulus of the t' corresponding to the zeros diverge as $L\to\infty$. Consequently, provided L for is sufficiently large, the zeros lie in a region where $u_+>\alpha$. Guided by the wisdom coming from Sec. II A we can assume that the zeros accumulate onto a curve γ_L which separates the complex plane into two regions. In the first one, the behavior is dominated by the algebraic part and the integral in Eq. (37) is essentially $\int_{1/\Lambda_L}^{\alpha}h(u,t')du\sim[1/(\tau-1)][\Lambda_L^{\tau-1}-\alpha^{\tau-1}]$. In the second region, the exponential part dominates. Provided t' is sufficiently large ($u_+\gg\alpha$), the variations of $u^{-\tau}g(u)$ are small compared to the increase of $e^{t'u}$ and this function can be approximated by some constant Γ_g. Hence $\int_{u_-}^{\alpha}h(u,t')du\sim\Gamma_g\int_{u_-}^{\alpha}e^{t'u}du\sim(\Gamma_g/t')[e^{t'\alpha}-e^{\tau}]$.

Consequently, for sufficiently large L, the zeros are well approximated by

$$\frac{1}{t'}[e^{t'\alpha}+a_1t'-a_2]=-\frac{\Lambda_L^{\tau-1}}{\Gamma_g(\tau-1)}, \tag{38}$$

where $a_1=\alpha^{\tau-1}/\Gamma_g(\tau-1)$, $a_2=e^{\tau}$.

This equation is similar to Eq. (19). The zeros are now given by

$$t_L(k)=-\frac{W_k\left(\dfrac{\alpha\Gamma_g(\tau-1)}{\Lambda_L^{\tau-1}}\right)}{\alpha\Lambda_L}. \tag{39}$$

Consequently, one finds that the pattern of zeros in the finite-size scaling case is essentially the same as the power law case, up to a correction depending on α,Γ_g. More precisely, using the series expansion (21) of the Lambert function one finds

$$\mathrm{Re}[t_L(k)]\sim\frac{-\log\left(\dfrac{\alpha\Gamma_g(\tau-1)}{\Lambda_L^{\tau-1}}\right)+\dfrac{1}{2}\log\left[\log^2\left(\dfrac{\alpha\Gamma_g(\tau-1)}{\Lambda_L^{\tau-1}}\right)+4k^2\pi^2\right]}{\alpha\Lambda_L}, \tag{40}$$

$$\mathrm{Im}[t_L(k)]\sim\frac{2k\pi}{\alpha\Lambda_L}, \tag{41}$$

where $k=1,\ldots,\xi_L=\alpha\Lambda_L$.

In the z plane this essentially results in a trivial rescaling of the argument $\mathrm{Im}[t_L(k)]$ and a slight change in the modulus $R_L(k)$,

$$R_L^{FSS}(k)\sim\kappa_L R_L^{PL}(k)^{1/\alpha}, \tag{42}$$

where the superscript FSS (PL) refers to the finite size scaling (power law) situation. $\kappa_L=(1/\alpha\Gamma_g)^{1/\alpha\Lambda_L}$ is therefore a scaling factor which tends to 1 as expected since the zeros have to accumulate on the unit circle. In Eq. (42) we neglected the more complicated dependence coming from the log(log) term. This has a small effect on the first zeros but becomes negligible as k grows. This provides a way to determine κ_L. Setting $R_L^{PL}(\pi)$ for the farthest zero from $z=1$,

$$\kappa_L=\frac{R_L^{FSS}(\pi)}{R_L^{PL}(\pi)^{1/\alpha}}. \tag{43}$$

The argument of $t_L(k)$'s is

$$\arg[t_L(k)]\sim\arctan\left(\frac{2k\pi}{-\log\left(\frac{\alpha\Gamma_g(\tau-1)}{\Lambda_L^{\tau-1}}\right)+\frac{1}{2}\log\left[\log^2\left(\frac{\alpha\Gamma_g(\tau-1)}{\Lambda_L^{\tau-1}}\right)+4k^2\pi^2\right]}\right). \tag{44}$$

The cutoff g modifies, therefore, the value of the angles but *not the scaling*.

We numerically checked these result in the following case. We generated a probability distribution given by

$$P_L(n)=C_L n^{-\tau} g\left(\frac{n}{L^\beta}\right), \quad n=1,\ldots,\alpha L^\beta \tag{45}$$

where

$$g(x)=e^{-x^\gamma}. \tag{46}$$

We fixed the parameters to the values $\beta=2,\tau=1.9,\gamma=2.5,\alpha=1$. We show in Fig. 5 the collapse of the curve of zeros to the corresponding curve for a power law with the same τ,β. κ was computed from the ratio (43). We found $\kappa=1.0001$ for $L=100$.

3. Effect of a sampling cutoff

We would like now to point out a very simple way to violate the scaling form (30) by the only numerical procedure traditionally used in the computation of $P_L(n)$. This effect is closely related to the anomalous scaling of the Lee-Yang zeros since it appears for a critical exponent $\tau>1$.

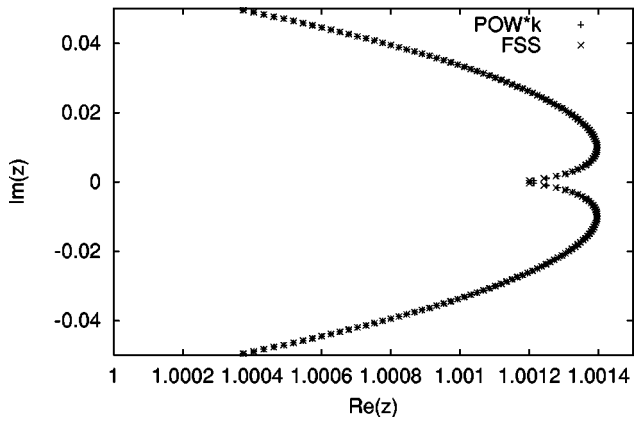

FIG. 5. Pattern of zeros in the z complex plane for the power law case, $\beta=2,\tau=1.9,L=100$, where the real and imaginary part have been multiplied by κ, and for the FSS case $\beta=2,\tau=1.9,\gamma=2.5,\alpha=1,L=100$.

In numerical simulations, one computes an empirical distribution $P_L^{exp}(n,\omega)=\mathcal{N}(n,\omega)/\mathcal{N}$ where $\mathcal{N}$ is the total number of avalanches observed during the simulation and $\mathcal{N}(n,\omega)$ is the number of times an avalanche of size n was observed. This number is a random variable depending, say, on the initial condition(s), or more generally, on the seed ω used in the random generator. However, one expects the system to be ergodic in a strong sense such that $P_L^{exp}(n,\omega)\to P_L(n)$ as $\mathcal{N}\to\infty$ for generic choices of ω (see [10] for details.). However, since $\mathcal{N}$ is finite, there exists wild fluctuations in the tail of the distribution. Furthermore, the avalanches such that $P_L(n)<1/\mathcal{N}$ have a small (though nonzero[7]) probability to be observed in a numerical simulation and this probability decreases as n increases. Obviously, there are several methods such as smoothing or binning, allowing us to reduce the effects of noise in the tail.

There exists, however, another more subtle effect. In all the examples of numerical computations that we have found in the SOC literature, the value of $\mathcal{N}$ is fixed, *independently of the system size*. This induces a pathological bias affecting the extrapolation to the thermodynamic limit whatever the method used to analyze the empirical distribution. In particular a violation of finite-size scaling can be observed on $P_L^{exp}(n,\omega)$ *even if the theoretical probability* $P_L(n)$ *obeys Eq. (30). When* $\mathcal{N}$ *is kept fixed while* L increases, the estimation of the maximal value ξ_L that the random variable can take (defining the exponent β) is more and more biased. Indeed, while the true ξ_L diverges as $L\to\infty$, the empirical value $\xi_L^{exp}(\omega)$ converges to a constant. Consequently, the probability distribution extrapolated to the thermodynamic limit from the empirical distribution is biased. The aim of this section is to analyze this effect, which not discussed in the literature.

[7]However, since the largest nonzero value of $P_L^{exp}(n,\omega)$ is $1/\mathcal{N}$, the events such that $P_L(n)\ll 1/\mathcal{N}$, even when observed, are given an incorrect probability by the numerical procedure. The discrepancy with the theoretical value increases as n increases.

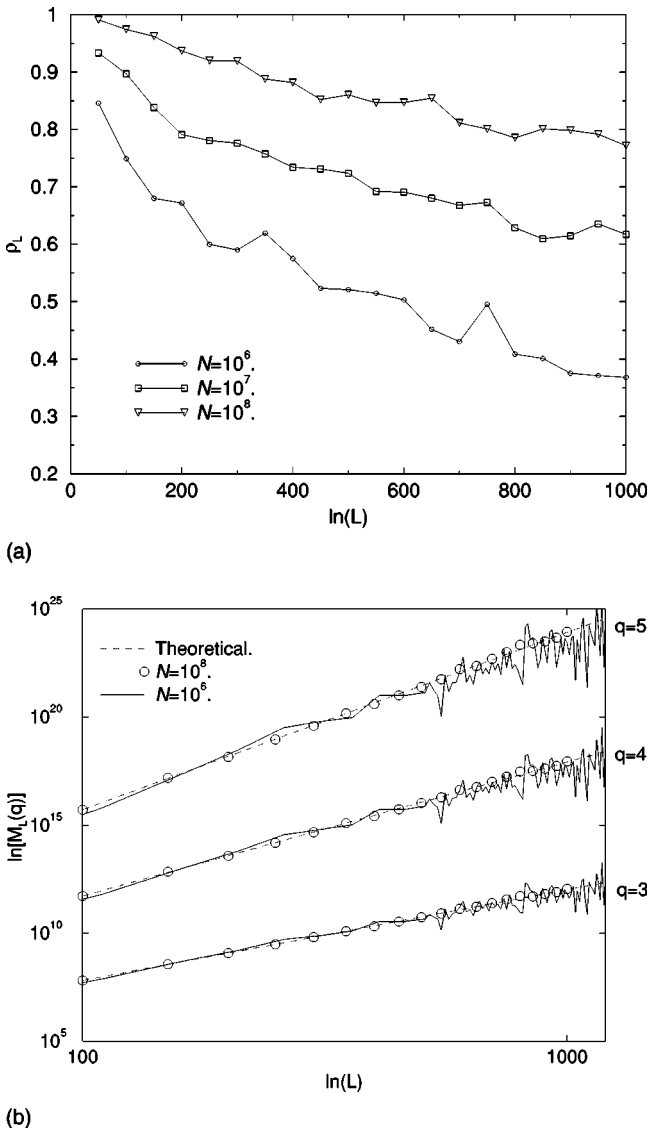

FIG. 6. Effect of the sampling cutoff. (a) Ratio $\rho_L = E[\xi_{L,\mathcal{N}}^{exp}]/\xi_L$. (b) Moments.

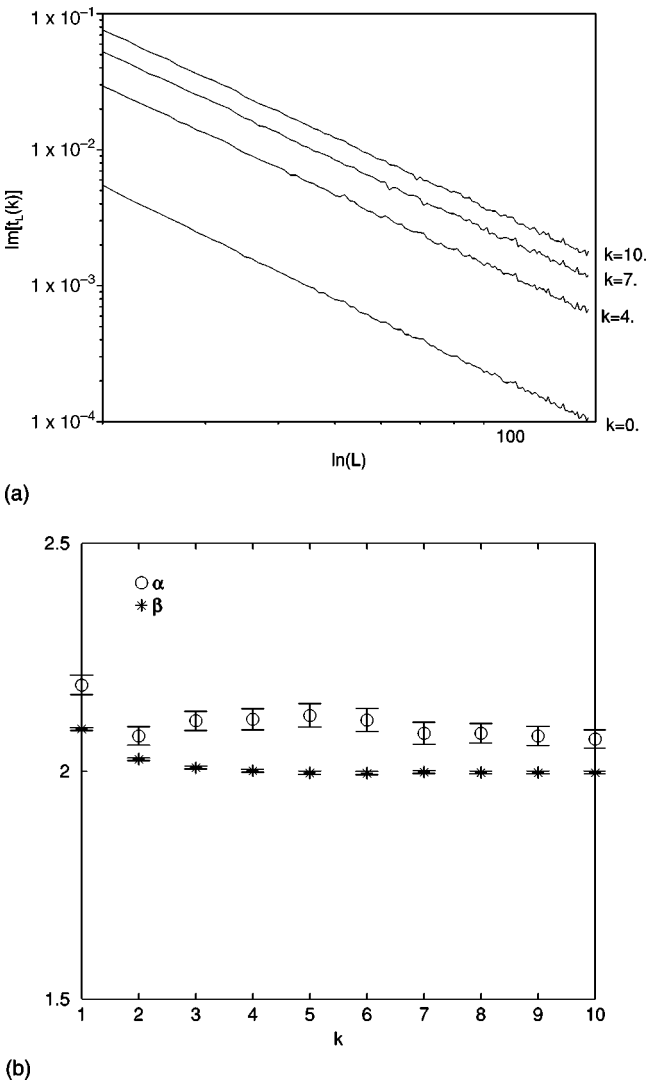

FIG. 7. (a) Argument of the first Lee-Yang zeros of an empirical distribution generated from $\mathcal{N}=10^8$ samples. (b) Values of α,β extrapolated from (a).

Assume therefore that $P_L(n)$ is like Eq. (29) with a cutoff obeying Eq. (30). We call $F_L(n)=\Sigma_{k=1}^{n}P_L(k)$ the corresponding repartition function. Assume now that we perform a finite sampling of the probability distribution with $\mathcal{N}$ trials $X_1,\ldots,X_{\mathcal{N}}$, where $X_i, i=1,\ldots,\mathcal{N}$ are independent,[8] identically distributed random variables, with probability $P_L(n)$. Assume, furthermore, that $\mathcal{N}$ is fixed independently of L. Call $\xi_{L,\mathcal{N}}^{exp}=\max\{X_k,k=1,\ldots,\mathcal{N}\}$ the maximal value observed in the finite sampling. The repartition function of the random variable $\xi_{L,\mathcal{N}}^{exp}$ is $F_L^{\mathcal{N}}(x)$. Its average is given by

$$E[\xi_{L,\mathcal{N}}^{exp}]=\xi_L-\sum_{n=1}^{\xi_L}F_L^{\mathcal{N}}(n). \tag{47}$$

Clearly, were L fixed while $\mathcal{N}\to\infty$, then $E[\xi_{L,\mathcal{N}}^{exp}]$ would converge to ξ_L. In fact the ergodic theorem gives a stronger statement, namely $\xi_{L,\mathcal{N}}^{exp}\to\xi_L$ almost surely in this case. This essentially means that for sufficiently small L, $E[\xi_{L,\mathcal{N}}^{exp}]$ gives a good estimate of ξ_L. On the other hand, if $\mathcal{N}$ is fixed while L increases, the correction term $\Sigma_{n=1}^{\xi_L}F_L^{\mathcal{N}}(n)$ in Eq. (47) becomes more and more important, leading to a wrong estimation of ξ_L. To be more precise fix a value $y\in]0,1[$, such that $F_L^{\mathcal{N}}$ is considered as non-negligible as soon as $F_L^{\mathcal{N}}(n)>y$. Hence y is somehow arbitrary here (say close to 0). Since $F_L^{\mathcal{N}}(n)$ is strictly increasing the equation $F_L^{\mathcal{N}}(x)=y\Leftrightarrow F_L(x)=y^{1/\mathcal{N}}$ has a unique solution $x_L\equiv x_L(y)$, $\forall y\in]0,1[$. If L is small (or if $\mathcal{N}$ is sufficiently large) $x_L\sim\xi_L$ and therefore $F_L^{\mathcal{N}}(n)$ is essentially nonzero for $n\sim\xi_L$. In this case the term $\Sigma_{n=1}^{\xi_L}F_L^{\mathcal{N}}(n)$ in Eq. (47) is negligible compared to ξ_L.

On the other hand, x_L is bounded from above by a *finite* value x such that $F^*(x)=K\Sigma_{n=1}^{x}n^{-\tau}=y^{1/\mathcal{N}}$, where F^* is the repartition function of the limiting probability $P^*(n)$. Con-

[8]We assume here that the trials are independent for simplicity. In SOC models the avalanches are not independent, though for finite L the correlation decay can be fast (it is exponential in the finite size Zhang model).

sequently, as L increases, for any $y \in]0,1[$, $x_L(y)/\xi_L \to 0$. Hence, the function $F_L^{\mathcal{N}}(x)$ is non-negligible on a larger and larger interval, whose length scales like ξ_L. Therefore, the sum $\Sigma_{n=1}^{\xi_L} F_L^{\mathcal{N}}(n)$ in Eq. (47) becomes more and more important, yielding a decrease in the expectation of the empirical maximum.

In the range of L values where this effect starts to manifest one has $x_L \sim \xi_L$. Hence, $\Sigma_{n=1}^{\xi_L} F_L^{\mathcal{N}}(n) \sim \Sigma_{n=x_L}^{\xi_L} F_L^{\mathcal{N}}(n)$ and $F_L^{\mathcal{N}}(n)$ has only to be estimated in the interval $[x_L, \xi_L]$. Furthermore, $F_L(n) = 1 - \Sigma_{k=n}^{\xi_L} P_L(n) \sim 1 - C_L \int_n^{\xi_L} u^{-\tau} g(u/\Lambda_L) du$. When x_L is close to ξ_L, $\int_n^{\xi_L} u^{-\tau} g(u/\Lambda_L) du \sim (\xi_L - n) \xi_L^{-\tau} g(\alpha)$ for $n \in [x_L, \xi_L]$. Furthermore, in this range, $1 - C_L \xi_L^{-\tau} (\xi_L - n) g(\alpha)$ is small compared to 1. Hence, $F_L^{\mathcal{N}}(n) \sim 1 - \mathcal{N} C_L \xi_L^{-\tau} (\xi_L - n) g(\alpha)$. The equation $F_L^{\mathcal{N}}(x) = y$ has therefore an approximate solution $x_L = \xi_L - [(1-y)/\mathcal{N} C_L g(\alpha)] \xi_L^{\tau}$. Then $\Sigma_{n=1}^{\xi_L} F_L^{\mathcal{N}}(n) \sim \Sigma_{n=x_L}^{\xi_L} F_L^{\mathcal{N}}(n)$ can be roughly approximated by a linear interpolation giving $\Sigma_{n=x_L}^{\xi_L} F_L^{\mathcal{N}}(n) \sim (\xi_L - x_L)/2 = [(1-y)/\mathcal{N} C_L g(\alpha)] \xi_L^{\tau}$.

Consequently, the empirical expectation is in this approximation

$$E[\xi_{L,\mathcal{N}}^{exp}] \sim \xi_L \left(1 - \frac{1-y}{\mathcal{N} C_L g(\alpha)} \xi_L^{\tau-1} \right). \tag{48}$$

Since $\tau > 1$ the correction term increases as L grows. It eventually becomes of the same order as ξ_L, but when L increases one has to add higher order corrections to Eq. (48). On the other hand, were $\tau < 1$, then would the correction term become negligible as L grows.

The L value where the effect starts can be estimated by

$$L \sim \left(\frac{1-y}{\mathcal{N} C_L g(\alpha)} \right)^{-1/\beta(\tau-1)}. \tag{49}$$

Consequently, this effect is more prominent when $\beta(\tau-1)$ is larger.

The ratio $\alpha_L = E[\xi_{L,\mathcal{N}}^{exp}]/L^{\beta}$ is therefore not equal to a constant α as it must be, but is L dependent [see Fig. 6(a)]. Clearly, for sufficiently large L *the corresponding probability violates the finite size scaling and the data collapse*. Furthermore, the scaling of the moments is also affected by this effect. Indeed the moments are obtained empirically from the formula $m_L^{exp}(q) = \Sigma_{n=1}^{\xi_L^{exp}} n^q P_L^{exp}(n)$ and the scaling exponents are extrapolated from the formula

$$\sigma^{exp}(q) = \lim_{L \to \infty} \frac{\log[m_L^{exp}(q)]}{\log(L)}.$$

When L is sufficiently small, $\xi_L^{exp} \sim \alpha L^{\beta}$ since the correction due to the finite sampling has essentially no effect. Then one obtains the right scaling exponent $\sigma(q)$ from the data. However, when L increases, one observes *a spurious deviation of the curve $m_L(q)$ from the theoretical value*. This effect is illustrated in Fig. 6 in the case $\tau = 1.9, \beta = 2, \gamma = 2.5, \alpha = 2$, $g(x) = e^{-x^{\gamma}}$ where two samples with $\mathcal{N} = 10^6$ and $\mathcal{N} = 10^8$ were generated. Note that the effect is more prominent when q increases.

This computation shows therefore that for the values $\tau > 1$ numerical problems appear, induced by the finite size sampling. Not only the fluctuations of $\xi_{L,\mathcal{N}}^{exp}$ increase but also the averaged value $E[\xi_{L,\mathcal{N}}^{exp}]$ is biased. To our opinion, the estimation of the correct ξ_L is the main problem in analyzing the data from SOC simulations.

The analysis of the Lee-Yang zeros for relatively small sizes can, however, give a fairly good estimate of the values α, β allowing to extrapolate ξ_L to larger size. Indeed, Eq. (40) suggests that the argument of $t_L(k)$ is not too sensitive to the fluctuations of $\xi_{L,\mathcal{N}}^{exp}$ [compared to the fluctuations of the moments which are of order $(\xi_{L,\mathcal{N}}^{exp})^{q+1-\tau}$]. Hence, it is possible to find the values of α, β. We give an example in Fig. 7 where the empirical data are the same as those used for the computation of the moments. As for the truncated power law, we found a slight deviation for the first zero. Interpolating the values from $k = 1, \ldots, 10$ we found $\alpha = 2.094 \pm 0.006 \pm 0.09, \beta = 2.002 \pm 0.003$ which gives quite a good estimate.

The real part of Lee-Yang zeros and, consequently, the argument, is more sensitive to nonextensive sampling effect. An analytical expression is obtained if one modifies the equations (22)– (24) by replacing α by α_L. The argument of $t_L(k)$ writes now

$$\arg[t_L(k)] \sim \arctan\left(\frac{2k\pi}{-\log\left(\frac{\alpha_L \Gamma_g(\tau-1)}{\Lambda_L^{\tau-1}} \right) + \frac{1}{2} \log\left[\log^2\left(\frac{\alpha_L \Gamma_g(\tau-1)}{\Lambda_L^{\tau-1}} \right) + 4k^2\pi^2 \right]} \right). \tag{50}$$

The finite sample effect is illustrated Fig. 8 for the first zero. One observes a deviation from the real curve for $\mathcal{N} = 10^6$. This can be used as an empirical way to define the L where the empirical distribution is not biased. Note that the curve of the argument of the first empirical zero obtained for $\mathcal{N} = 10^8$ follows the theoretical curve with a good accuracy. This shows that the determination of the zeros is robust with respect to fluctuations in the coefficients of the polynom (1). This is in fact an easy consequence of the implicit function theorem.

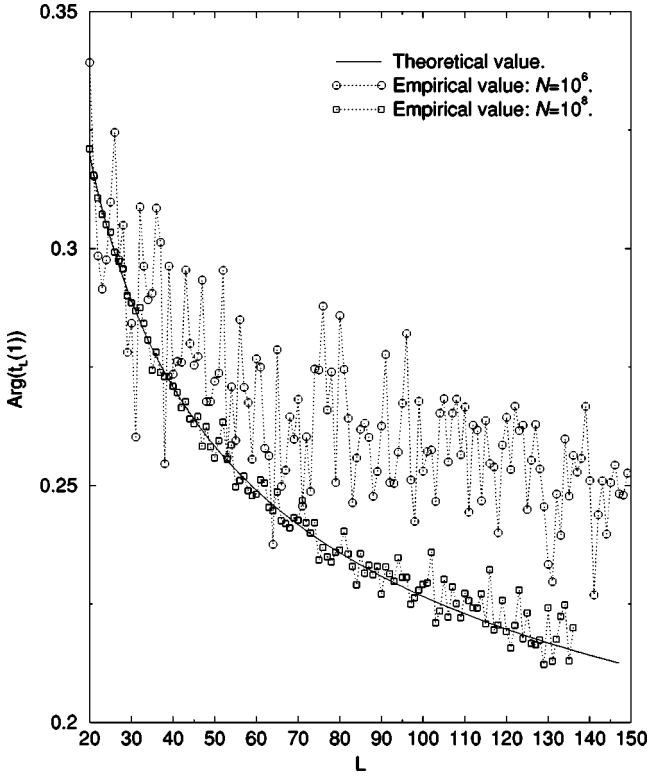

FIG. 8. Effect of a sample cutoff on the argument of the zeros in the t plane.

Looking at Figs. 6(b) and 8 one could argue that the moments are less sensitive than the Lee-Yang zeros to a size independent sampling. However, the sensitivity of the moments increases with the degree q. Therefore, to detect this effect, one has to compute the moments for high q. This can clearly cause numerical problems. On the other hand, the Lee-Yang zeros integrate information about all order moments and the sensitivity can be detected easily. We believe that this kind of analysis is prior to any investigation concerning in particular the multifractal nature of the scaling.

Our conclusion is therefore twofold. Firstly, some cautions are required when increasing L to extrapolate the thermodynamic limit. If $\mathcal{N}$ is kept fixed, *too large* L will give *wrong* estimations. In this case at least, the bigger is not the best. This effect can be compared to the critical slowing down in the literature about critical phenomena. However, to the best of our knowledge we do not know any example in the SOC literature where this effect has been discussed. Secondly, the Lee-Yang zeros nevertheless give useful information. They can be used to determine the range of L values where the data are not too affected, and, in this range, the simple scaling of the imaginary part allows us to determine the scaling of ξ_L. This can be used with other methods such as binning, or smoothing, to determine the exact distribution from the empirical one.

4. Other scaling

In this section we investigate briefly the other scaling forms discussed in Sec. II B. Our main conclusion is that the Lee-Yang zeros are highly sensitive to the changes in the scaling form. This remark opens the perspective to develop a general theory allowing us to extrapolate the characteristics of probability distributions from the behavior of the Lee-Yang zeros of the empirical generating function. However, we have not yet been able to provide an equivalent of the analytic forms Eqs. [(20) and (39)] that would be helpful to properly extract the features of the probability distribution from the Lee-Yang zeros. The development of such a general framework is under investigation and will be published in a separated paper. We give a few numerical examples in Figs. 9(a) and 9(b).

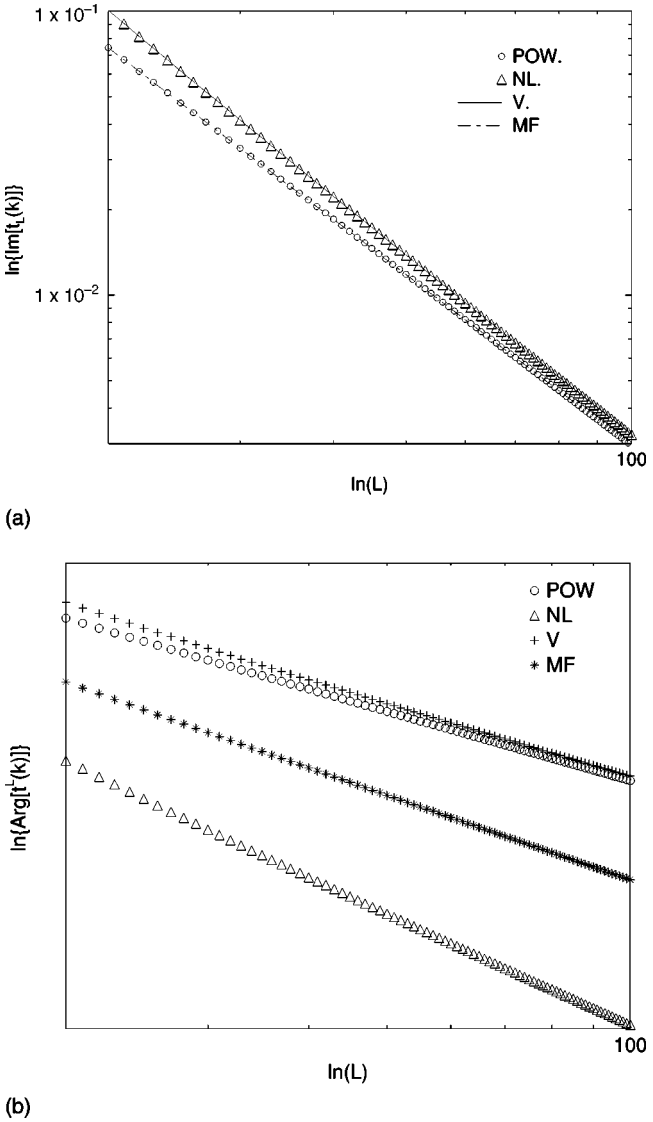

FIG. 9. (a) Argument $\theta_L(5)$ for the truncated power law (POW), a truncated power law with L-dependent β (V), a probability distribution of the form (33) with $F_L(x)$ given by Eq. (51) (NL), and a multifractal distribution (MF). (b) Argument of $t_L(5)$.

We investigated first the case (33) where $F_L(x)=Y(x-\beta_L)$. In this case, the computations done in Sec. II A essentially hold, with a β depending on L. In particular, Eq. (26) suggests that the L dependence of β should be detected on the argument of $z_L(k)$, $\theta_L(k)$. In Fig. 9, we plotted $\theta_L(5)$ in the case $\beta_L=\beta[1-(1/L)]$, where $\beta=2,\tau=1.9$, and L

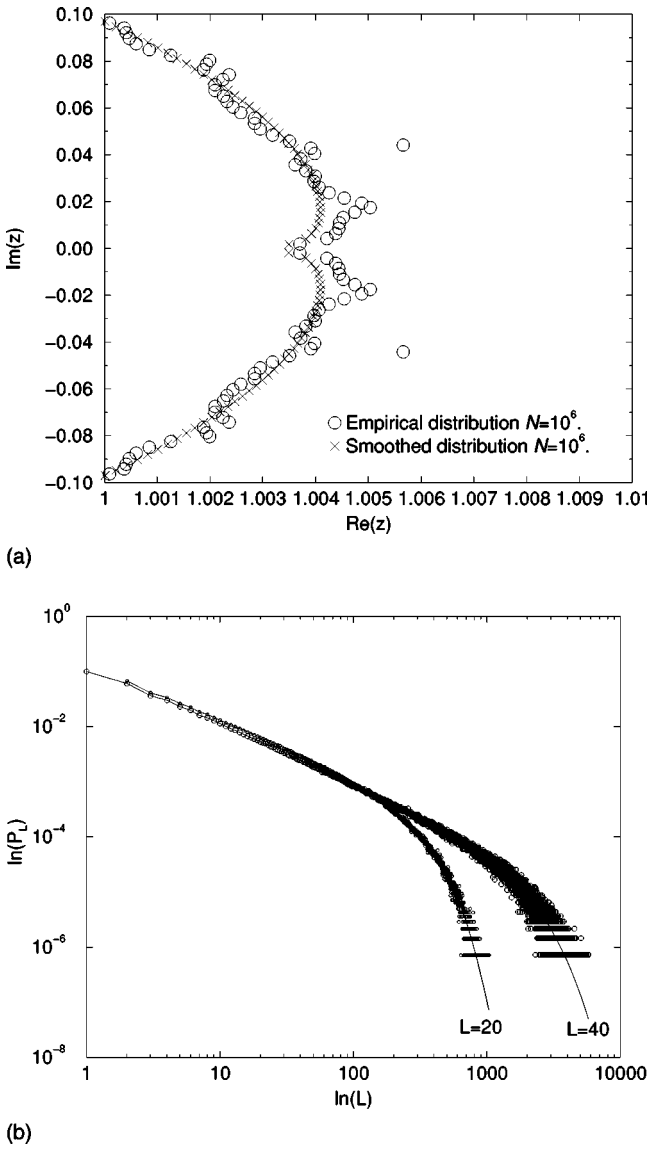

FIG. 10. (a) Zeros in the z plane for $L=30$, $\epsilon=0.1$, $\mathcal{N}=10^6$, $E_c=2.2$. The zeros of the experimental, $\mathcal{N}=10^6$, and smoothed probability distribution are represented. (b) Examples of empirical and smoothed probability distributions used in the computation of the zeros.

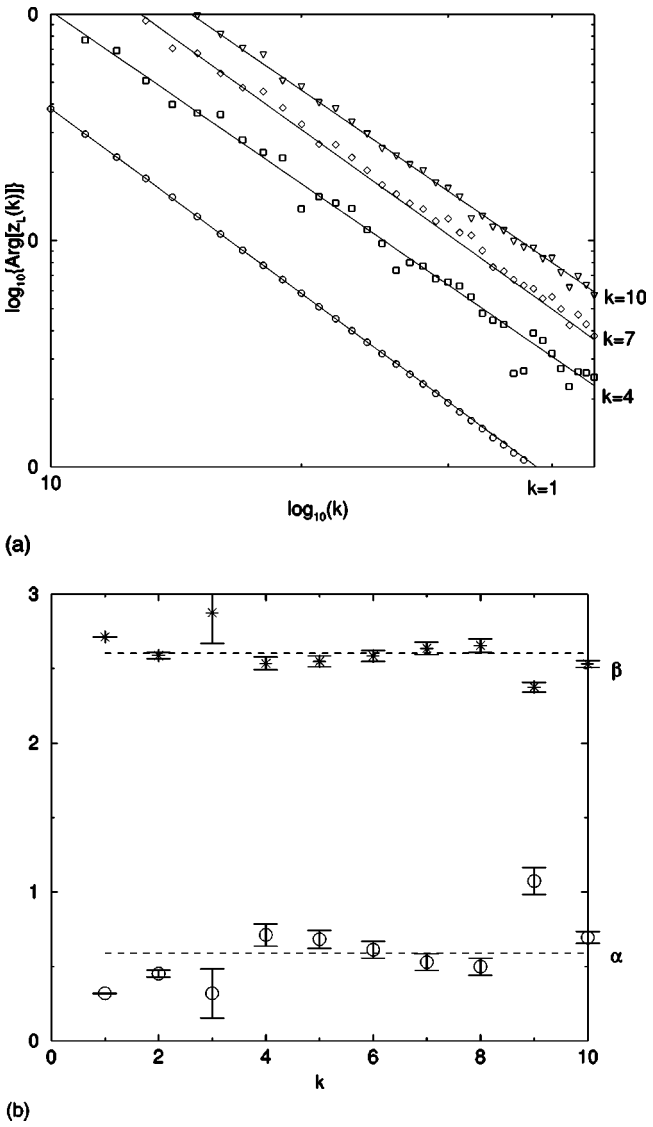

FIG. 11. (a) Argument of the five first Lee-Yang zeros in the z plane versus L for $Ec=2.2,\epsilon=0.1$. The full lines corresponds to a fit. (b) Plot of the fit parameters α,β versus k.

$=20,\ldots,120$. The theoretical prediction is $\theta_L(5)=10\pi/L^{\beta[1-(1/L)]}$. We tried a fit of the form $f(x)=10\pi/L^{\beta[1-(1/L^{\alpha})]}$, where α,β are the fit parameters. We found $\alpha=1.014(8)\pm0.0006,\beta=2.013(9)\pm0.0001$, which is quite satisfactory.

We also tried a more general form for $F_L(x)$ with a nonlinear F_L converging to a step function as $L\to\infty$,

$$F_L(x)=-\left\{1+\tanh\left[L^{\alpha_1}\left(x-\beta-\frac{1}{L^{\alpha_2}}\right)\right]\right\},\quad x\leqslant\beta-\frac{1}{L^{\alpha_2}}. \tag{51}$$

In our simulations, $\beta=2,\tau=1.9,\alpha_1=0.1,\alpha_2=1$. L^{α_1} controls the rate of approach of $F_L(x)$ to the step function as L grows. A small α_1 gives a slow convergence and therefore has an effect up to very large L.

The result for the argument $\theta_L(5)$ is also represented in Fig. 9a. We note that the curve is indistinguishable from the previous case and therefore the imaginary part of t_L is not sensitive to the nonlinear effect of the tanh, but gives the right α_2. On the other hand, we noted that the argument of t_L is sensitive to the nonlinear effect [Fig. 9(b)].

For the multifractal case we studied the case where the multifractal spectrum has the form $f(x)=C-\tau x-ax^2$. This is the lowest degree nonlinear form of f compatible with (i) and (ii) and with the convexity of f. The values of $\alpha=1,\beta=2,\tau=1.9$ were the same as for the previous examples. We observe [Fig. 9(a)] that $\theta_L(k)$ is not sensitive to the multifractality and gives therefore the right α,β. Consequently, our method to estimate the degree is also valid for a multifractal distribution (32). On the other hand, $\arg[t_L(k)]$ is modified for a multifractal distribution, but we are not yet

able to analyze this variation. All the results are depicted in Fig. 9(a) ($\theta_L(5)=\mathrm{Im}[t_L(5)]$) and Fig. 9(b) ($\arg[t_L(5)]$).

III. AN EXAMPLE OF A SOC MODEL

In this section we study an example of the Lee-Yang zeros computation for a SOC model, the Zhang model, defined as follows. Let Λ be a d-dimensional sublattice in $\mathbb{Z}^d$, taken as a square of edge length L for simplicity. Call $N=\#\Lambda=L^d$, and let $^{\partial}\Lambda$ be the boundary of Λ, namely the set of points in $\mathbb{Z}^d\backslash\Lambda$ at distance 1 from Λ. Each site $i\in\Lambda$ is characterized by its ''energy'' X_i, which is a non-negative real number. Call $\mathbf{X}=\{X_i\}_{i\in\Lambda}$ a configuration of energies. Let E_c be a real, strictly positive number, called the *critical energy*, and $\mathcal{M}=[0,E_c[^N$. A configuration $\mathbf{X}$ is called ''stable'' if $\mathbf{X}\in\mathcal{M}$ and ''unstable'' otherwise. If $\mathbf{X}$ is stable then one chooses a site i at random with probability $1/N$, and add to it energy δ (excitation). If a site i is *over critical* or *active* ($X_i\geqslant E_c$), it loses a part of its energy in equal parts to its $2d$ neighbors (relaxation). Namely, we fix a parameter $\epsilon\in[0,1[$ such that the remaining energy of i is ϵX_i, after relaxation of the site i, while the $2d$ neighbors receive the energy $(1-\epsilon)X_i/2d$. Note, therefore, that the energy is locally conserved. If several nodes are simultaneously active, the local distribution rules are additively superposed, i.e., the time evolution of the system is synchronous. The succession of updating leading an unstable configuration to a stable one is called an *avalanche*. The energy is dissipated at the boundaries of the system, namely the sites of $^{\partial}\Lambda$ have always zero energy. As a result, all avalanches are *finite*. Consequently, whatever the observable n, $\xi_L<\infty$ for finite L. The addition of energy is *adiabatic*. When an avalanche occurs, one waits until it stops before adding a new energy quantum. Further excitations eventually generate a new avalanche, but, because of the adiabatic rule, each new avalanche starts from *only one* active site. It is conjectured that a critical state is reached in the thermodynamic limit.

Though it has long been believed that the Zhang model obeys finite size scaling (30), a recent paper revised this point of view and claimed that the Zhang model does not even have a multifractal scaling (but no alternative scaling was proposed [15]). We will not solve this debate in this paper. Rather we will come to two conclusions. First, because of high sensitivity of the model to the sample cutoff (Fig. 12), one has somehow to relativize the conclusions about the scaling obtained from the numerical simulations. This shows that to draw any reliable conclusion on the scaling one has to increase *the sample with the system size* (e.g., like L^{β}). This will clearly be rapidly intractable even for the fastest computers. Secondly, the Lee-Yang zeros give rather reliable extrapolations provided the size L is not too large.

We computed the empirical probability distribution of avalanche sizes $P_L^{exp}(s)$ where the size is the total number of relaxing sites during one avalanche. We did our simulations for lattice sizes from $L=10$ to $L=55$ in two dimensions, with $E_c=2.2,\epsilon=0.1$ with a statistics over $\mathcal{N}=10^6$ and $\mathcal{N}=10^8$ avalanches. Consequently, $\mathcal{N}$ was fixed *independently of* L as usually done in SOC numerical simulations.

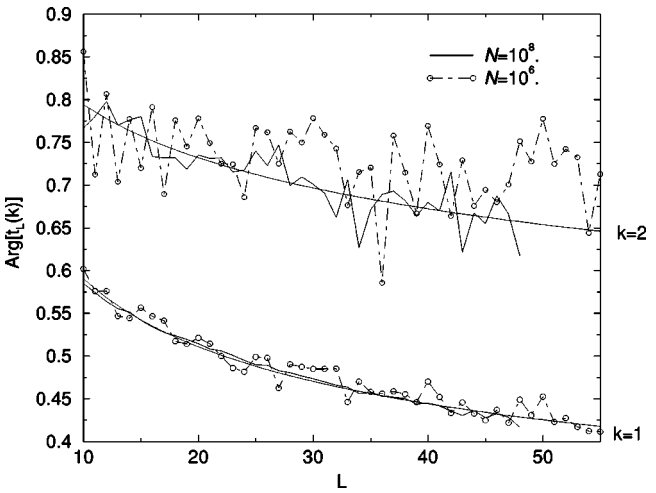

FIG. 12. Argument of Lee-Yang zeros $t_L(1),t_L(2)$ for $Ec=2.2,\epsilon=0.1$. Full lines indicate the interpolation of the empirical curves obtained from the sampling with $\mathcal{N}=10^8$.

We first present in Fig. 10(a) the experimental zeros in the z complex plane for $L=30$, $\mathcal{N}=10^6$. In order to see the effect of the noise, we also computed the zeros of a smoothed version of the empirical probability distribution [Fig. 10(b)]. The smoothing method uses a binning procedure, followed by a spline extrapolation, allowing us to fill the ''holes'' existing in the empirical probability distribution. These holes correspond to events that did not happen during the trial and consequently are given a zero probability. In the numerical computation of the zeros, these holes correspond, therefore, to vanishing coefficients in the polynom (1), which produce problems in the convergence of most of the root finding algorithms. Our numerical procedure seems, however, to be robust with respect to this effect.

As argued all along in this paper, the argument $\theta_L(k)$ provides a way to determine the exponent β characterizing the maximal avalanche size. We plot in Fig. 11(a) the $\theta_L(k)$'s for $k=1,\ldots,5$ versus L. We note that $\theta_L(k)$ is quite robust to noise and gives therefore a reliable way to measure β,α. We used a fit form $2\pi k/\alpha L^{\beta}$, where α,β are fit parameters. We found a slight k dependence for the first zeros [as expected from Eq. (23) if one assumes FSS]. We plotted in Fig. 11(b) the extrapolated α,β versus k. For $k>3$ these values seem to stabilize around $\alpha=0.62\pm0.07$ and $\beta=2.59\pm0.04$. In the finite size scaling ansatz β and τ are related by $\beta(2-\tau)=2$ [25] and $\tau=1.253$ is known from the renormalization group analysis. Therefore the predicted value for β is 2.667. Despite the smallness of the L we considered, the computed value is not too far from the predicted one. However, an accurate determination of β,τ and a precise check of FSS would demand somewhat larger size systems, which we were unable to generate for this illustration. (Note that the main problem is not the computation of the zeros, since there exist quite fast and precise root finding algorithms, but the generation of P_L^{exp} itself.)

Finally, we investigate the scaling of the argument $t_L(k)$ and a possible size independent sampling effect. The main difficulty here is the wild fluctuations in ξ_L^{exp}. Indeed, the

real part of $t_L(k)$ is more sensitive than the imaginary part to these fluctuations and consequently $\arg[t_L(k)]$ as wild fluctuations. Only the first zeros seem to be robust to this effect. As discussed in Sec. II B 3 these fluctuations in ξ_L^{exp} are intrinsic to the empirical computation of P_L^{exp} and cause problems in the extrapolation to the thermodynamics limit, whatever the method used. We plotted in Fig. 12 the argument of the two first Lee-Yang zeros in the t plane, versus L. Our simulations suggests that the Zhang model is sensitive to the size independent sampling. Note in particular that the values of L that we used in our computation are quite smaller that the ones found in the literature and the effect is already significant for $\mathcal{N} \leqslant 10^6$.

This shows clearly that a reestimation of the conclusions drawn from the numerics in the Zhang model (and also, maybe, for some other SOC models) should be done in light of this effect. On the other hand, our approach suggests that there may be no need to go to gigantic sizes provided the finite lattice size effects are carefully handled. From this point of view, analytic formulas like Eq. (44) might provide a way to analyze these effects.

CONCLUSION

In this paper we have shown that the finite size study of the SOC-like probability distributions leads to similar Lee-Yang or Fisher phenomenon as in statistical physics models near the critical point. This implies that the convergence of the SOC state to a critical state with power law statistics can be analyzed in a similar way as equilibrium statistical mechanics. More precisely, the way the zeros of the partition function accumulate on the real axis, when the size of the system grows up, provides relevant informations on the critical structure of the observed system. In particular, it permits us to measure useful critical indices of the underlying theory.

Moreover, we have shown that the size of the SOC models power exponent, $\tau > 1$, leads to a comprehensive violation of the standard scaling laws. We give a approximate theory of this effect well confirmed by numerical simulations. It is the same characteristic which leads to a specific sensibility of the SOC numerical experiments to size independent sampling effects. We studied carefully this effect on extrapolation to the limit $L \to \infty$ and show that it could possibly mimic important effects such as multifractality. We notice that the argument of the zeros in the $t = \log(z)$ plane is a good test of this effect.

We show that the arguments of the first zeros in the z plane of the generating function, $G(z)$, is rather insensitive to these effects, statistically robust, and provides a nice way to compute the SOC α and β parameters. Using the standard Kadanoff *et al.* scaling form [13], we verify that the parameter's values as extracted from numerical simulations were in good agreement with the theoretical input of the model. This last result gives us some confidence to extract the values of these parameters from Zhang's model numerical data. Notice that these results have been extracted from medium range simulations. This shows up once more for the power of the finite size analysis of the critical phenomenon.

This paper is (with [20]) a first step toward the scaling theory of the SOC system from the behavior of the Lee-Yang zeros. The next step would be the definition of the exponents characterizing the approach to criticality, like the exponents α, β, γ in statistical mechanics and their link to the scaling of the zeros.

ACKNOWLEDGMENTS

This work has been partially supported by the Zentrum fuer Interdisciplinaere Forschung (ZIF) of Bielefeld (Germany), in the frame of the project ''The Sciences of Complexity: From Mathematics to Technology to a Sustainable World.'' B.C. warmly acknowledge the ZIF for its hospitality. He also thanks the CNRS for its support. He is grateful to Ph. Blanchard, T. Krueger, P. Bak, and M. Paczuski for illuminating discussions while in Bielefeld. We also thank G. Batrouni and K. Bernardet for computer facilities and useful references.

[1] P. Bak, C. Tang, and K. Wiesenfeld, Phys. Rev. Lett. **59**, 381 (1987); Phys. Rev. A **38**, 364 (1988).
[2] P. Bak, *How Nature Works* (Springer-Verlag, Berlin, 1996).
[3] H.J. Jensen, *Self-Organized Criticality : Emergent Complex Behavior in Physical and Biological Systems*, Cambridge Lecture Notes in Physics Vol. 10 (Cambridge University Press, Cambridge, 1998).
[4] P. Bak and C. Tang, Phys. Rev. Lett. **60**, 2347 (1988).
[5] D. Sornette, A. Johansen, and I. Dornic, J. Phys. I **5**, 325 (1995).
[6] D. Dhar, Phys. Rev. Lett. **64**, 1613 (1990); D. Dhar and S.N. Majumdar, J. Phys. A **23**, 4333 (1990); S.N. Majumdar and D. Dhar, Physica A **185**, 129 (1992); D. Dhar and R. Ramaswamy, Phys. Rev. Lett. **63**, 1659 (1989).
[7] H.Y. Zhang, Phys. Rev. Lett. **63**, 470 (1988).
[8] Ph. Blanchard, B. Cessac, and T. Krüger, J. Stat. Phys. **88**, 307 (1997).
[9] B. Cessac, Ph. Blanchard, and T. Krueger, *Mathematical Results in Statistical Mechanics*, Marseille, 1998 (Word Scientific, Singapore, 1998).
[10] Ph. Blanchard, B. Cessac, and T. Krüger, J. Stat. Phys. **98**, 375 (2000).
[11] D. Ruelle, *Statistical Mechanics: Rigorous Results* (Benjamin, New York, 1969).
[12] C. Maes, F. Redig, E. Saada, and A. Van Moffaert, Markov Processes Relat. Fields **6**, 1 (2000).
[13] L.P. Kadanoff, S.R. Nagel, L. Wu, and S. Zhou, Phys. Rev. A **39**, 6524 (1989).
[14] C. Tebaldi, M. De Menech, and A. Stella, e-print cond-mat/9903270.
[15] R. Pastor-Satorras and A. Vespignani, Eur. Phys. J. B **18**, 197 (2000); eprint cond-mat/0010223.
[16] S. Lise and M. Paczuski, Phys. Rev. E **63**, 036111 (2001); e-print cond-mat/0008010.

[17] C.N Yang and T.D. Lee, Phys. Rev. **87**, 404 (1952); **87**, 410 (1952).
[18] W. Janke and R. Kenna, J. Stat. Phys. **102**, 1221 (2001).
[19] R.J. Creswick and S.Y. Kim, Phys. Rev. E **56**, 2418 (1997).
[20] B. Cessac, Ph. Blanchard, T. Krüger, and J. L. Meunier (unpublished).
[21] Ya.G. Sinai, Russ. Math. Surveys **27**, 21 (1972).
[22] D. Ruelle, *Thermodynamic Formalism* (Addison-Wesley, Reading, Mass., 1978).
[23] R. Bowen, *Equilibrium States and the Ergodic Theory of Anosov Diffeomorphisms*, Lecture Notes in Mathematics Vol. 470 (Springer-Verlag, Berlin 1975).
[24] G. Keller *Equilibrium States in Ergodic Theory* (Cambridge University Press, Cambridge, 1998).
[25] B. Cessac, Ph. Blanchard, and T. Krüger, Phys. Rev. E **64**, 016133 (2001).
[26] S. Grossmann and W. Rosenhauer, Z. Phys. **218**, 138 (1967).
[27] R. Abe, Prog. Theor. Phys. **38**, 1 (1967).
[28] M. Suzuki, Prog. Theor. Phys. **38**, 1225 (1967).
[29] V. Privman and M.J. Fisher, Phys. Rev. B **30**, 1 (1984).
[30] C. Itzykson, R.B. Pearson, and J.B. Zuber, Nucl. Phys. B: Field Theory Stat. Syst. **220[FS8]**, 415 (1983).
[31] M.L. Glasser, V. Privman, and L.S. Schulman, Phys. Rev. B **33**, 1 (1987).
[32] C.M. Newman, *Constructive Quantum Field Theory*, edited by G. Velo and A.S. Wightman (Springer-Verlag, Berlin, 1973), pp. 321–325; C.M. Newman, Commun. Pure Appl. Math. **27**, 143 (1974); Commun. Math. Phys. **41**, 1 (1975).
[33] J. Salas and A.D. Sokal, e-print cond-mat/0004330; A.D. Sokal, Physica A **279**, 324 (2000).
[34] M. Biskup, C. Borgs, J.T. Chayes, L.J. Kleinwaks, and R. Kotecky, Phys. Rev. Lett. (to be published), e-print math-ph/0004003.
[35] D. Ruelle, e-print math-ph/0009030.
[36] R.M. Corless, D. Jeffrey, and D.E. Knuth, in Proceedings of ISSAC '97, Maui, pp. 197–204; R.M. Corless, G.H. Gonnet, D.E.G. Hare, D.J. Jeffrey, and D.E. Knuth, Adv. Comput. Math. **5**, 329 (1996); D.J. Jeffrey, D.E.G. Hare, and Robert M. Corless, Math. Scientist **21**, 1 (1996).
[37] J. Salas and A.D. Sokal, J. Stat. Phys. **88**, 567 (1997).
[38] Ph. Ruelle and Ph. Sen, J. Phys. A **25**, 1257 (1992).